SMITHSONIAN CONTRIBUTIONS TO THE EARTH SCIENCES • NUMBER 25

Inclusions in the Allende Meteorite

Brian Mason
and S.R. Taylor

SMITHSONIAN INSTITUTION PRESS
City of Washington
1982

ABSTRACT

Mason, Brian, and S.R. Taylor. Inclusions in the Allende Meteorite. *Smithsonian Contributions to the Earth Sciences*, number 25, 30 pages, 25 figures, 5 tables, 1982.—Six discrete groups of inclusions have been distinguished in the Allende meteorite. Groups I, V, and VI are mostly melilite-rich chondrules, although some have been extensively altered to fine-grained aggregates; Groups II and III are mostly fine-grained aggregates made up largely of spinel and fassaite; Group IV are olivine-rich aggregates and chondrules. Each group has a distinctive trace-element pattern, most clearly shown by the rare-earth (RE) distribution pattern. Group I has an unfractionated pattern (except for a small positive Eu anomaly) at about 10–15 times chondrites; Group II has a highly fractionated pattern with depletion of the heavier lanthanides (Gd-Er) and negative Eu and positive Tm and Yb anomalies; Group III has an unfractionated pattern at about 20 times chondrites, except for negative Eu and Yb anomalies; Group IV has a relatively unfractionated pattern at 2–4 times chondrites; Group V has an unfractionated pattern at 10–20 times chondrites; Group VI has an unfractionated pattern at 10–20 times chondrites, except for positive Eu and Yb anomalies (i.e., complementary to Group III). The complex patterns of trace element distribution in these Allende inclusions indicate a complex history of formation of this meteorite from the solar nebula.

OFFICIAL PUBLICATION DATE is handstamped in a limited number of initial copies and is recorded in the Institution's annual report, *Smithsonian Year*. SERIES COVER DESIGN: Aerial view of Ulawun Volcano, New Britain.

Library of Congress Cataloging in Publication Data
Mason, Brian Harold, 1917–
Inclusions in the Allende meteorite.
(Smithsonian contributions to the earth sciences ; no. 25)
Bibliography: p.
1. Allende meteorite. I. Taylor, Stuart Ross, 1925–. II. Title. III. Series.
QE1.S227 no. 25 [QB756.A44] 550s [523.5'1] 82-600091 AACR2

Contents

Inclusions in the Allende Meteorite

Brian Mason
and S.R. Taylor

Introduction

The fall of the Allende meteorite in northern Mexico on 8 February 1969 was a unique event in the history of meteoritics. One of us (BM) was in the field immediately after the event, and even a cursory examination of the first specimens recovered showed that the meteorite was a Type 3 carbonaceous chondrite but with components never before seen—notably giant chondrules (Figure 1) which proved to have a remarkable mineral association (melilite-titanian fassaite-spinel-anorthite) and white to pink irregular aggregates. The Smithsonian Institution field party collected about 150 kg of meteorites and distributed material to scientists in 37 laboratories in 13 countries within a few weeks of the date of fall. Clarke et al. (1970) published an account of the field occurrences and gave a comprehensive account of the morphology and composition of the meteorite. They distinguished the following major components: (a) matrix, (b) chondrules, (c) irregular aggregates, (d) dark inclusions. The chondrules were divided into two groups on the basis of chemical and mineralogical composition: (I) Mg-rich olivine, sometimes with clinoenstatite and interstitial glass (similar to the common chondrules in Type 3 meteorites), and (II) Ca- and Al-rich chondrules (first recognized as a significant component in Allende, although a similar chondrule had previously been described (Christophe Michel-Lévy, 1968) from the Vigarano C3 chondrite). Chemical analyses were given of the bulk meteorite, matrix, Mg-rich chondrules, two Ca,Al-rich chondrules, a Ca,Al-rich aggregate, and a dark inclusion.

The availability of large amounts of Allende and the concurrent distribution of lunar samples resulted in extensive and intensive research on this meteorite, so that the literature on Allende now probably outweighs that on any other meteorite. Researchers have concentrated on the Ca,Al-rich inclusions (both chondrules and aggregates), partly because their compositions suggest that they might be early condensates from solar nebula and partly because of the isotopic anomalies recognized therein (first oxygen (Clayton, Grossman, and Mayeda, 1973) and later other elements). Research on other components, however, has not been neglected; see, for example, publications on dark inclusions (Fruland et al., 1978) and on Mg-rich chondrules (Simon and Haggerty, 1980).

The useful acronym CAI has been widely adopted to refer collectively to Ca,Al-rich chondrules and aggregates in Allende (and other C3 meteorites). Its use obviates the sometimes subjec-

Brian Mason, Department of Mineral Sciences, National Museum of Natural History, Smithsonian Institution, Washington, D.C. 20560. S.R. Taylor, Research School of Earth Sciences, Australian National University, Canberra, A.C.T., Australia 2600.

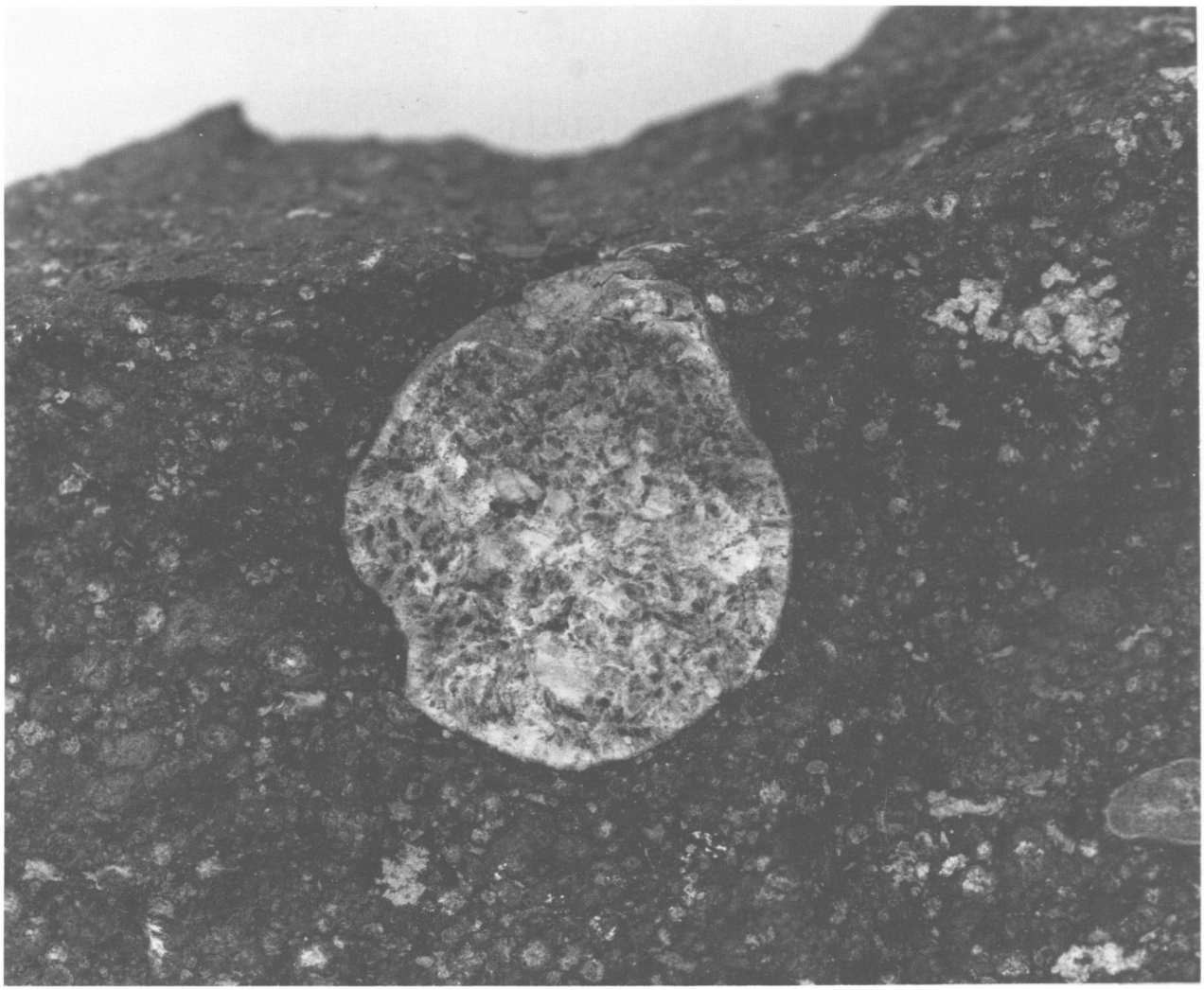

FIGURE 1.—Allende 3529-G, a melilite-fassaite-spinel-anorthite chrondrule, 25 mm in diameter; note the size contrast with the small (~1 mm) olivine-rich chondrules in the surrounding matrix.

tive judgment whether a specific inclusion crystallized as a molten droplet (possibly plastically deformed and/or fragmented) or originated as an aggregate of solid particles.

ACKNOWLEDGMENTS.—We thank Ms. P. Oswald-Sealy, Mr. J.M.G. Shelley, and Mr. N. Ware for assistance in the analytical work. One of us (BM) enjoyed the hospitality of the Max-Planck-Institut für Kernphysik and the advice and help of Dr. A. El Goresy during part of this research. The Smithsonian Research Foundation contributed part of the costs of the research, and this contribution is gratefully recorded.

Experimental Methods

A large number of Allende specimens in the collections of the National Museum of Natural History (NMNH) were inspected, and those showing prominent and readily extractable chondrules and aggregates were selected for detailed examination. From these, over 40 chondrules and

aggregates have been extracted and subjected to complete chemical and mineralogical analysis, and many others investigated to a lesser degree. We point out, however, that our selection was biased towards the larger and more easily extracted inclusions and cannot be considered as statistically representative of the total variety of Allende inclusions. This has been clearly demonstrated by the work of Kornacki (1981). He identified 189 fine- to medium-grained inclusions in 17 Allende thin sections but found none of the melilite-rich chondrules on which so much research has been published. Most of our inclusions were extracted from NMNH 3529, a 32-kilogram stone; in this stone, as in most Allende specimens, the inclusions are irregularly distributed, as can be seen in Figure 2. This figure shows that some pieces from a single stone may contain one or more of these large melilite-rich chondrules, whereas others have none. Each piece of Allende that we examined had many CAIs that were too small for our planned investigation.

As far as possible the CAIs were extracted from the matrix by simple mechanical tools and handpicking to avoid introducing contaminants; however, in some instances methylene iodide was used to separate the denser matrix from the less dense CAIs. Mineral identification and analysis were carried out using microscope, X-ray diffraction, and electron microprobe techniques. Compositional data for major elements and some minor elements were obtained by microprobe analyses of glasses prepared by fusion. The trace element data were obtained by spark source mass spectrometry (SSMS), using the procedures described by Taylor (1965, 1971) and Taylor and Gorton (1977). The precision is about ±5% and the accuracy about ±5%, but they vary somewhat, being poorer for elements below mass number 105 than for those of higher mass number. Recent data show ±2% agreement with isotope dilution mass spectrometric data for Sm and Nd. Some trace elements could not be determined because their concentrations were below the sensitivity of the technique. Among the lanthanides, Lu was not determined because of its use as an internal standard. The single mass number (169) for Tm is subject to interference from a multiple carbon ion, and this element cannot be accurately determined at low concentrations (<0.3 ppm). The 169 line, however, was unexpectedly strong in Group II samples, indicating the presence of a positive Tm anomaly. The rare earth (RE) data were normalized to chondritic abundances given by Taylor and Gorton (1977).

The platinum-group elements, normally below detection limit in the SSMS technique, were accessible in these samples. After extensive testing and calibration, the following mass numbers were found to provide reliable analytical data: ^{101}Ru, ^{103}Rh, ^{106}Pd, ^{185}Re, ^{190}Os, ^{191}Ir, and ^{195}Pt. All other mass numbers had various interferences.

Results

The results of our chemical analyses are summarized in Table 1. In the discussions which follow, these results are combined with the data on 20 Allende CAIs published by Mason and Martin (1977). They determined major and minor elements in 17 CAIs from the Allende meteorite and distinguished three groups on the basis of RE distribution patterns: Group I (10 melilite-fassaite-spinel-anorthite chondrules) had unfractionated chondrite-normalized RE distribution patterns at 10–15 times chondritic abundances with a positive Eu anomaly; Group II (5 aggregates) with La-Sm abundances similar to Group I but with rapidly diminishing abundances of the heavier RE, except for a positive Tm anomaly; Group III (2 aggregates) with unfractionated RE abundances about 20 times those of chondrites, except for large negative Eu and Yb anomalies. (Group IV comprised olivine-rich chondrules and aggregates with relatively unfractionated RE abundances at about three times chondrites; CaO and Al_2O_3 are relatively low (<10%), and hence Group IV samples are not discussed in this paper.) Taylor and Mason (1978) analyzed 18 CAIs (Table 1) and extended this classification with Group V (unfractionated RE distributions with no significant anomalies) and Group VI (RE

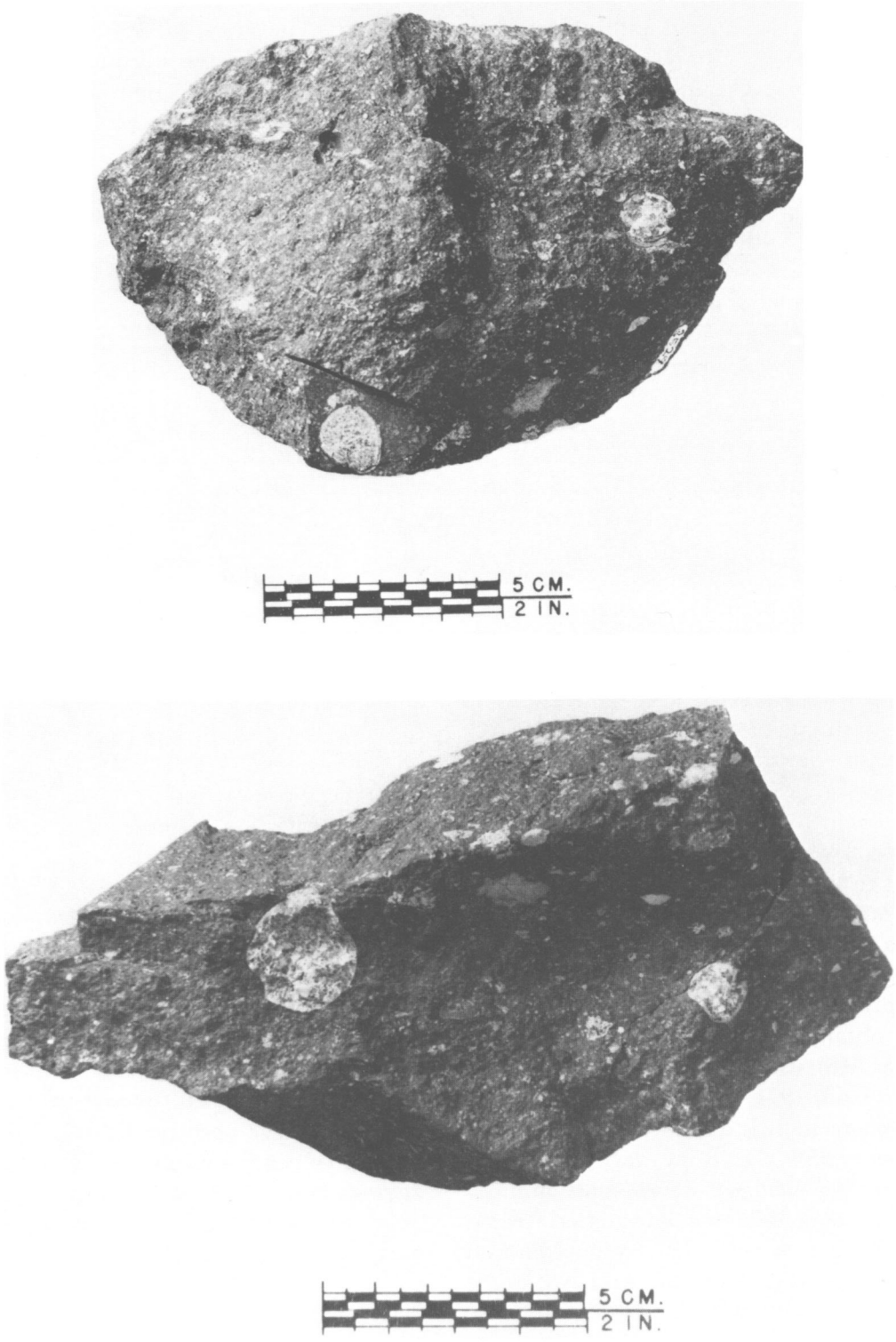

FIGURE 2.—Four pieces of Allende 3529, illustrating the irregular distribution of large CAI chondrules, CAI aggregates, and dark inclusions.


5 CM.
2 IN.

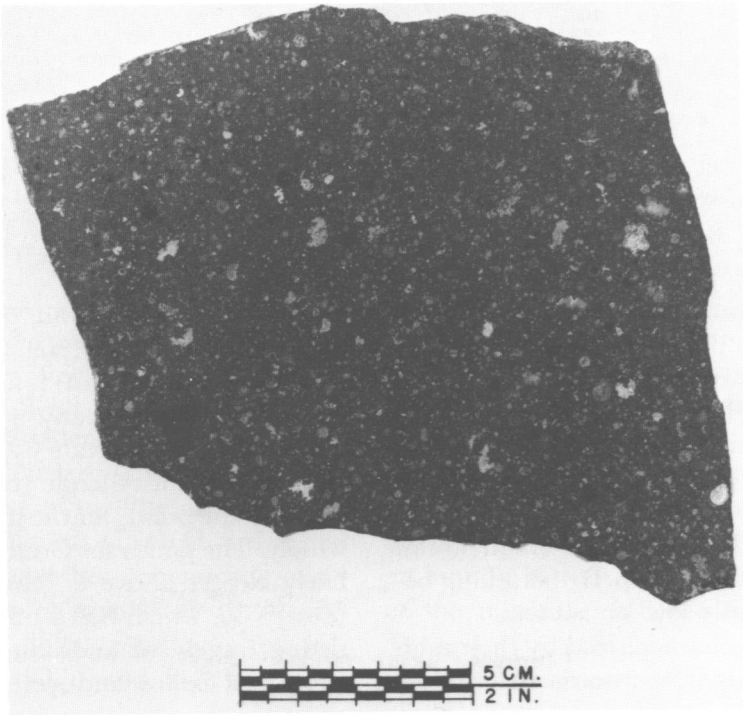
5 CM.
2 IN.

TABLE 1.—Analytical data on Allende CAIs by group and sample (4-digit sample numbers are NMNH catalog numbers; letters and 2-digit sample numbers are individual CAIs from NMNH 3529)

Constituent	I	II						III				V				VI		
	Z	40	5284	3655B	43	4691	5242	O	42	41	46	21	3655A	3682	45	44	Y	47
								PERCENT										
SiO_2	30.86	20.46	29.70	32.76	23.58	19.75	35.05	26.46	17.95	26.67	26.44	27.35	29.51	29.58	26.34	27.57	30.31	32.78
TiO_2	1.21	0.57	0.58	0.98	0.58	1.64	0.66	2.32	0.79	1.63	2.33	1.27	1.78	1.42	1.38	1.34	1.50	1.13
Al_2O_3	28.85	52.35	39.40	35.95	42.0	41.86	23.90	36.25	51.14	37.12	36.03	33.15	29.68	27.66	34.26	35.56	28.72	27.10
FeO	0.30	5.80	4.47	2.63	7.90	0.73	13.18	3.52	2.15	0.98	3.13	2.43	1.00	4.10	1.82	1.12	0.87	7.94
MgO	9.25	11.39	11.29	9.83	17.29	7.54	12.76	8.86	11.53	14.24	7.46	11.62	11.36	10.71	4.05	6.05	10.79	9.77
CaO	29.35	6.78	12.54	17.20	7.67	28.41	14.01	22.94	16.26	19.19	24.10	23.93	26.49	26.28	32.04	27.95	27.59	20.54
Na_2O	0.18	2.67	1.96	0.57	1.46	0.18	0.44	0.21	0.28	0.21	0.46	0.25	0.19	0.22	0.07	0.37	0.23	0.62
								PARTS PER MILLION										
Ba	75	8.6	12.5	52	19	50	11	42	23	51	58	36	37	46.5	46	46	37	27
Pb	7.2	0.34	0.84	1.52	1.35	–	1.32	–	0.82	1.06	1.28	3.3	1.24	–	1.41	2.1	2.6	2.0
Th	0.58	0.88	0.72	0.57	0.65	1.57	0.21	1.10	0.35	0.66	1.66	0.55	0.62	0.52	0.64	0.39	0.48	0.71
U	0.09	–	0.030	0.025	0.033	0.17	0.057	0.10	0.041	0.10	0.13	0.12	0.092	0.093	0.11	0.095	0.20	0.43
Th/U	6.4	–	24.3	22.1	19.5	9.2	3.7	11	8.4	6.7	13	4.7	6.8	5.7	5.6	4.2	2.4	1.7
Zr	97	2.0	3.6	7.3	3.43	10.3	5.3	95	–	81	108	69	112	102	88	91	90	67
Hf	2.35	–	0.10	0.18	–	0.40	0.15	3.20	–	2.40	3.30	2.05	2.74	2.92	2.13	2.07	1.97	1.91
Zr/Hf	41	–	36	41	–	26	33	30	–	34	33	34	41	35	41	44	46	35
Nb	3.75	0.13	0.94	1.82	0.64	4.37	1.59	3.64	1.43	4.03	5.64	5.83	5.41	3.56	7.02	5.31	7.80	7.47
La	5.36	14.6	8.46	9.21	8.72	20.3	3.3	7.51	3.66	5.20	11.6	5.25	4.89	4.08	6.36	4.24	4.43	4.75
Ce	12.8	38.2	23.0	22.7	23.1	–	12.8	19.4	9.50	14.4	–	13.2	13.3	11.2	–	11.9	13.6	12.4
Pr	2.03	5.74	3.20	3.44	3.98	7.7	1.53	2.68	1.46	2.01	4.30	1.88	1.99	1.60	2.59	1.54	1.65	1.67
Nd	9.74	29.4	16.8	18.7	18.3	37.8	6.81	14.1	7.52	10.0	22.0	9.88	10.4	8.31	13.9	8.06	8.53	8.21
Sm	2.77	7.62	5.17	5.38	5.41	11.0	2.30	4.12	2.19	3.35	6.37	2.85	3.00	2.65	4.20	2.30	2.65	2.50
Eu	1.37	0.29	0.35	0.52	0.40	1.04	0.35	1.09	0.50	0.77	1.33	1.00	1.01	0.89	1.53	1.31	1.14	0.95
Gd	3.62	2.87	2.77	3.57	3.07	5.26	0.48	6.15	2.89	4.02	8.10	3.58	4.19	3.56	5.63	3.00	3.24	3.20
Tb	0.67	0.50	0.49	0.58	0.55	0.96	0.09	1.13	0.54	0.81	1.58	0.68	0.78	0.68	1.03	0.59	0.62	0.63
Dy	4.62	2.41	2.62	3.12	2.81	4.95	0.53	7.80	3.61	5.38	10.6	4.67	5.36	4.63	7.39	3.96	4.51	4.18
Ho	1.17	0.13	0.15	0.25	0.16	0.28	0.07	1.95	0.85	1.29	2.68	1.14	1.30	1.18	1.64	0.98	1.06	0.99
Er	3.55	0.14	0.12	0.28	0.18	0.37	0.18	5.94	2.60	4.00	7.74	3.30	4.12	3.97	4.30	3.00	3.45	2.94
Tm	0.45	1.04	0.80	0.74	0.88	1.92	0.38	0.85	0.37	0.60	1.11	0.48	0.62	0.47	0.73	0.39	0.46	0.45
Yb	3.38	0.014	0.58	1.36	0.36	3.25	1.10	4.52	1.67	3.45	5.29	3.02	3.85	2.80	4.2	3.42	4.44	4.59
Σ RE	52	103	64.5	69.9	68	–	29.9	77	37	55	–	51	55	–	–	45	50	48
Y	34.8	0.99	1.51	3.43	1.85	3.80	1.77	41	24	31	50	28.7	42	33	40	37	38	26
								RATIOS										
Eu/Eu*	1.34	0.20	0.29	0.37	0.30	0.42	–	0.69	0.64	0.66	0.57	1.0	0.88	0.90	1.0	1.54	1.22	1.0
La/Yb	1.6	1040	14.6	6.8	24	6.21	3.0	1.7	2.2	1.5	2.2	1.74	1.3	1.5	–	1.24	0.99	1.03
Eu/Yb	0.41	21	0.60	0.38	1.1	0.32	0.32	0.24	0.30	0.22	0.25	0.33	0.26	0.31	0.36	0.38	0.26	0.21
Y/Er	9.8	7.1	12.5	12.3	10.2	10.3	9.8	6.9	9.2	7.8	6.5	8.7	10.2	8.3	9.3	12.3	11.0	8.8
Zr/Y	2.8	2.0	2.4	2.1	1.85	2.7	3.0	2.3	–	2.6	2.2	2.4	2.7	3.1	2.2	2.5	2.4	2.6
								PLATINUM-GROUP ELEMENTS (PPM)										
Pt	7.8	–	0.98	0.62	0.72	–	0.76	10.7	24	12.9	10.9	18.7	11.8	11.3	10.7	20	15.1	14.8
Ir	7.4	–	0.87	0.35	0.37	–	0.66	8.0	19.8	11.4	8.8	9.33	10.7	4.48	12.6	8.4	9.1	7.9
Os	7.0	–	0.37	0.27	0.35	–	0.63	7.5	19	10.4	7.7	8.89	9.85	4.41	10.5	7.2	9.6	7.1
Re	0.57	–	–	–	–	–	–	0.52	1.50	0.84	0.90	0.75	0.80	0.37	0.94	0.57	0.97	0.62
Pd	1.00	–	0.42	0.21	–	1.00	0.82	1.55	0.55	0.84	1.75	1.27	1.17	1.42	2.29	1.10	1.85	1.34
Rh	1.09	–	–	0.15	0.34	0.86	0.21	0.91	2.01	1.37	0.82	2.54	1.15	1.85	0.91	2.84	1.32	1.51
Ru	8.9	–	1.27	0.73	1.23	1.86	1.56	8.86	28.4	15.1	13.3	16.2	13.3	8.6	20	15.3	10.7	12.3

patterns the reciprocal of Group III, about 15 times chondrites with positive Eu and Yb anomalies). They noted, however, that major and trace-element distributions for Groups I, III, V, and VI show many similiarities. The application of this RE classification is illustrated in Figure 3. The CAIs clearly cluster in discrete groupings; the only discrepancy is 4698, a Group III inclusion which plots among the Group II inclusions because of an anomalously low Yb content.

Since the CAIs are characterized by their high Ca and Al contents, it is of interest to examine this relationship in detail, especially since Ahrens and von Michaelis (1969) have shown that the Ca/Al ratio (by weight) is almost constant at 1.09 in chondrites and many achondrites. This relationship for the Allende CAIs is shown in Figure 4; the point for Allende (bulk) falls on the 1.09 line, but the points for the individual CAIs scatter widely. The points for Groups I, V, and VI cluster fairly closely above or just below the 1.09 line (except 36, which has a unique mineralogy consisting largely of andradite). Group II and III CAIs plot below and generally well away from

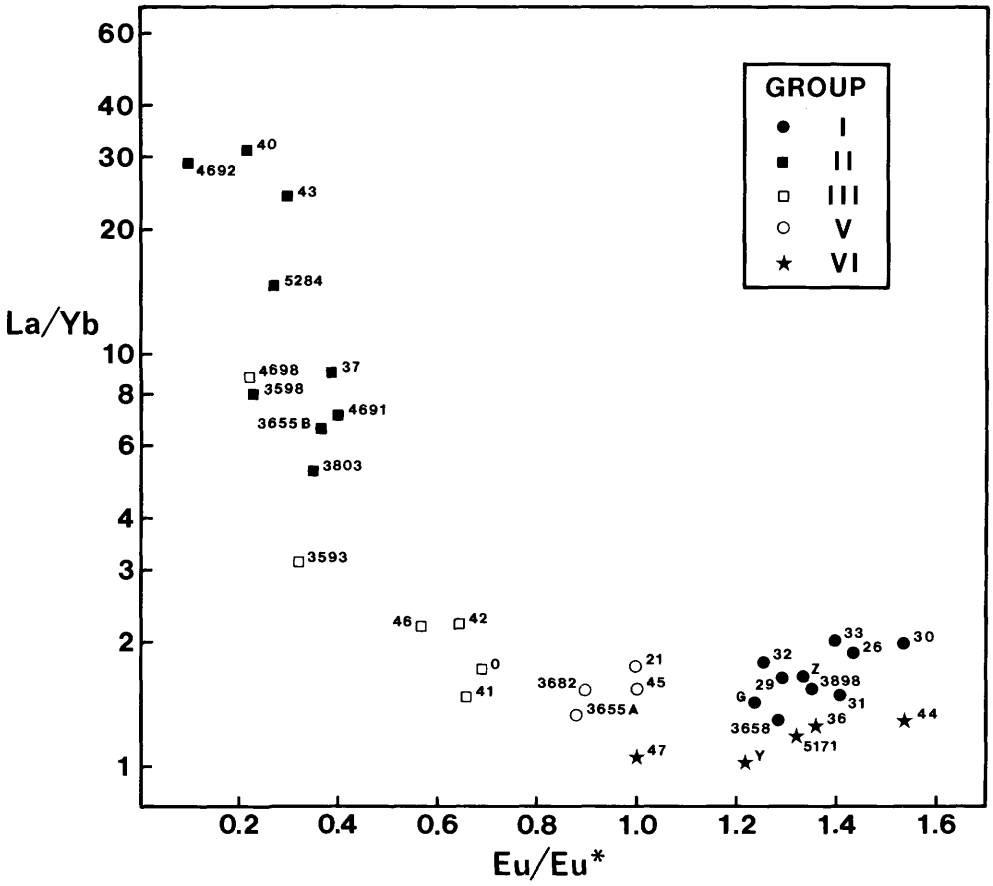

FIGURE 3.—Plot (semi-log) of La/Yb ratio vs. Eu/Eu* (europium anomaly) for Allende CAI groups (omitting Group IV) (4-digit sample numbers are NMNH catalog numbers; G, O, Y, Z, and 2-digit sample numbers are individual CAIs from NMNH 3529).

the 1.09 line and show a much wider range of Ca and Al contents than the other groups. The individual groups will now be discussed in detail.

GROUP I

Group I CAIs appear to be relatively restricted in chemical and mineralogical composition (Figures 3, 4) and are readily identified since they are all coarse-grained (grain size 0.5–3 mm) chondrules consisting largely of melilite and titanian fassaite, with minor amounts of spinel and anorthite (Figure 5). Ten have been chemically analyzed, of which the data on nine (3529-26, 29, 30, 31, 32, 33, G; 3658; 3898) were reported by Mason and Martin (1977), and for the tenth (3529-Z) the analytical data are given in Table 1 (5171, which was reported as a Group I CAI by Mason and Martin (1977) has been reclassified as Group VI). The RE data are summarized in Figure 6 for minimum (3529-31), average of 10, and maximum (3529-Z) values. RE data on CAIs by Gast, Hubbard, and Wiesmann (1970) and by Wänke et al. (1974) fall within the range of these Group I inclusions.

The mineralogical composition of the Group I inclusions is also relatively uniform. The data in Table 2 have been derived from microscopic examination of thin sections, microprobe analyses of the minerals, and the bulk compositions in Table 1. The principal variable in the mineralogical composition is the amount and composi-

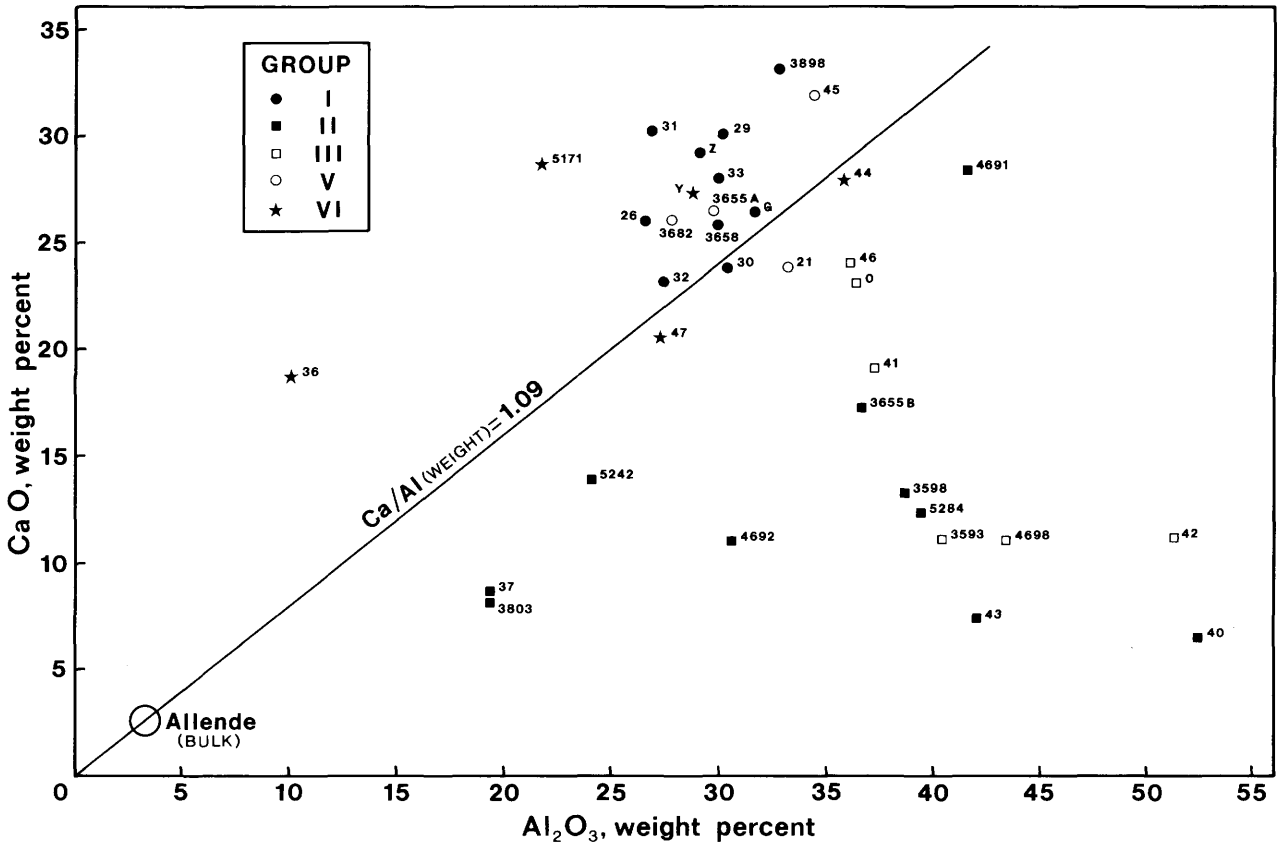

FIGURE 4.—The relationship between CaO and Al_2O_3 in individual samples (sample identifications as in Figure 3).

tion of the melilite. The pyroxene is highly aluminous (Al_2O_3, 16%–22%) and titanian (TiO_2, 3.9%–19.1%); a detailed account of these pyroxenes was published by Mason (1974). Spinel and anorthite have compositions close to stoichiometric $MgAl_2O_4$ and $CaAl_2Si_2O_8$. Melilite shows alteration along grain boundaries to a fine-grained material consisting largely of grossular, sometimes with minor nepheline; these minerals probably contain the minor amounts of FeO and Na_2O shown by the bulk analyses.

Two of these Group I inclusions (3529-29, 3898) contain minor amounts (<5%) of rhönite, whose unit-cell formula is $Ca_4X_{12}(Si, Al)_{12}O_{40}$, where X includes Mg, Fe, Ti, and Al. Rhönite and fassaite in 3529-29 are illustrated in Figure 7, and microprobe analyses of these minerals are given in Table 3. Rhönite in Allende CAIs is distinctly different from terrestrial rhönite in its high content of Al, Ti, and V and its low Si and Fe content. The high vanadium content is especially remarkable, since the content of this element in the bulk meteorite (90 ppm) is not exceptional. In meteoritic rhönite and fassaite the titanium is evidently present as both Ti^3 and Ti^4 (Dowty and Clark, 1973; Fuchs, 1978). In the formulas calculated from the analyses in Table 3, the titanium is arbitarily calculated as equal amounts of Ti^3 and Ti^4; this procedure results in excellent agreement with the structural formulas.

Figure 7 shows that the rhönite is rimmed and veined by black opaque material. This material has been described as a fassaite-spinel-perovskite symplectite by Haggerty (1977) and El Goresy, Nagel, and Ramdohr (1977). Haggerty interprets this symplectite as a decomposition product of

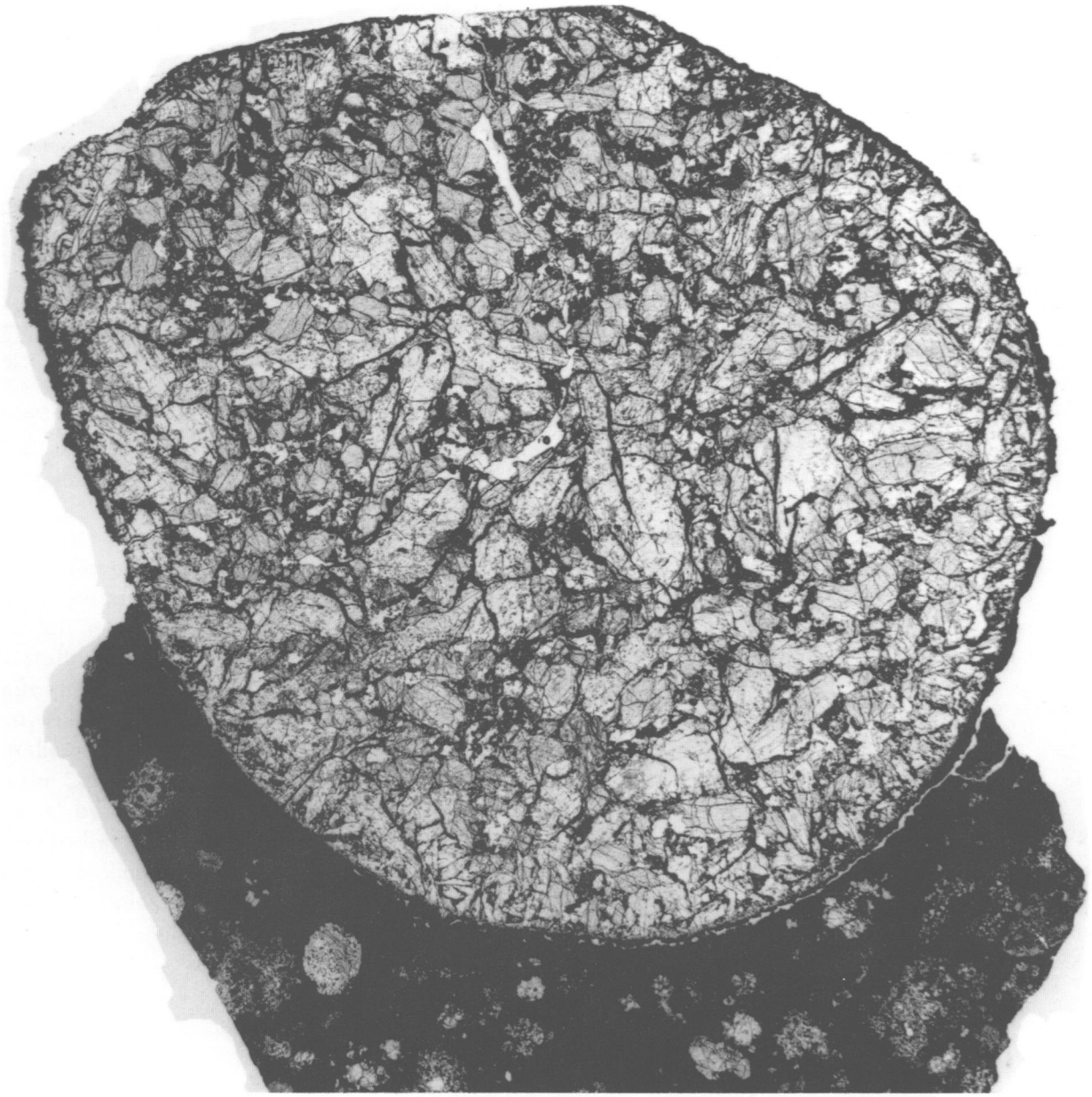

FIGURE 5.—Microphotograph (transmitted light) of 3529-G, a Group I melilite-rich chondrule 25 mm in diameter; melilite is present as large prismatic crystals, fassaite and anorthite occur as equant grains interstitial to the melilite, and spinel is disseminated as small grains throughout the other minerals.

rhönite, whereas El Goresy and his coworkers infer simultaneous precipitation of fassaite + perovskite from a silicate liquid around pre-existing rhönite and spinel. The Ca and Ti are present in rhönite in the correct proportions to produce perovskite in considerable amounts; some CAIs show patchy concentrations of perovskite grains suggestive of pre-existing rhönite.

Haggerty (1977:389) stated: "These cores (of rhönite) are unquestionably the earliest constitu-

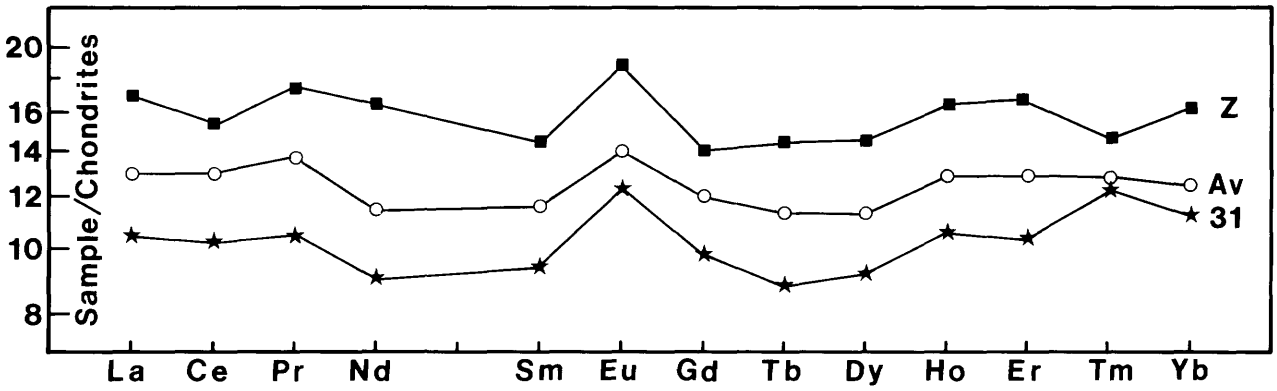

FIGURE 6.—RE distribution patterns for Group I CAIs (31 = minimum RE concentrations, Av = average of 10 Group I CAIs, Z = maximum RE concentrations).

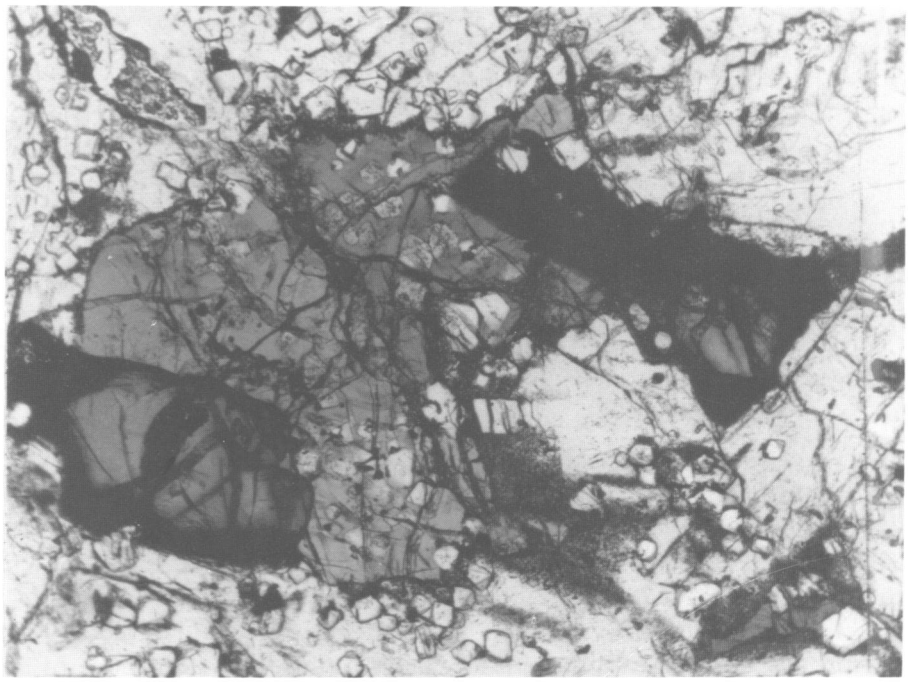

FIGURE 7.—Allende 3529-29: rhönite (darker gray, black borders) and fassaite (lighter gray) enclosed in melilite; idiomorphic spinel grains, average 0.05 mm, are present in melilite and fassaite.

TABLE 2.—Mineralogical composition of Group I inclusions (estimated weight percentages of minerals; range and mean Ak content of melilite)

Inclusion	Melilite	Fassaite	Spinel	Anorthite	Ak range and mean
3529-G	45	25	20	10	28–40, 34
3529-Z	50	25	15	10	18–43, 29
3529-26	50	25	5	20	11–65, 42
3529-29	60	15*	15	5	18–35, 26
3529-30	50	20	25	5	21–40, 28
3529-31	70	15	10	5	18–33, 24
3529-32	35	35	25	5	44–70, 65
3529-33	60	20	15	5	25–48, 31
3658	50	15	20	15	22–32, 28
3898	75	10*	10	5	13–25, 19

* Includes rhönite.

ent in the CAT (Ca-Al-Ti-rich inclusion)." Our observations suggest the reverse, that rhönite was the last mineral to crystallize. The sequence of crystallization appears to be spinel-melilite-fassaite-rhönite. As Clarke et al. (1970:39) pointed out, the sequence spinel-melilite-fassaite is that predicted from studies of crystallization of melts in the CaO-MgO-Al_2O_3-SiO_2 systems and is supported by textural relations in the melilite-rich chondrules, in which small euhedral crystals of spinel are included within all the other minerals; melilite is present as large zoned crystals (indicating crystallization over a considerable temperature interval), whereas fassaite occurs as smaller xenomorphic grains in the interstices of the melilite crystals. These relations are present in 3529-29 and 3898, with the rhönite enclosed in the fassaite. The extreme enrichment of Ti and V in the rhönite probably represents a concentration of these elements in the residual liquid after practically all the material of the chondrule had crystallized as spinel and melilite, both essentially free of these elements. Boivin (1980) has demonstrated that in terrestrial rocks rhönite is a late-crystallized phase, after spinel and pyroxene.

Data on some of these Group I inclusions have been reported in the literature. The ^{39}Ar–^{40}Ar systematics of 3529-Z have been studied by Herzog et al. (1980), who find it contains excess ^{40}Ar over that produced by in situ decay of ^{40}K. Niemeyer and Lugmair (1980) report the Ti isotopic composition in this inclusion. Jessberger et al. (1980) have published K-Ar data on 3529-26. El Goresy et al. (1979) have reported a number of accessory phases in "Fremdlinge" in 3529-29, including a calcium phosphate containing Mo and Ru, and Fe- and V-rich oxides; in this inclusion Jessberger et al. (1980) have reported K-Ar data, El Goresy and Ramdohr (1980) have reported Os depletion in "Fremdlinge," and Jordan et al. (1980) have found an unusual Xe isotopic composition. Mason and Martin (1974) separated melilite and pyroxene from 3529-32 and analyzed these minerals for major, minor, and trace elements; they recorded high contents of Mo and the Pt elements (except Pd) in both minerals and suggested that these elements were present as minute grains of native metal, a suggestion that

TABLE 3.—Rhönite and fassaite compositions in Allende inclusions (nd = not determined)

Constituent	1	2	3	4
SiO_2	15.58	16.12	30.50	30.23
TiO_2	23.15	19.80	18.64	19.05
Al_2O_3	28.38	28.57	21.19	20.27
Cr_2O_3	0.20	0.26	0.06	0.00
V_2O_3	3.09	3.32	0.83	0.85
FeO	0.18	2.80	0.03	0.05
MnO	0.02	0.03	0.04	0.02
MgO	15.18	14.97	5.68	5.85
CaO	13.86	14.07	23.80	23.74
Na_2O	nd	0.03	nd	0.02
Total	99.64	99.97	100.77	100.08

Column 1: Rhönite, 3529-29; calculated formula $Ca_{3.88}(Mg_{5.91}Ti^{3}_{2.27}Ti^{4}_{2.27}Al_{0.79}V_{0.65}Fe_{0.04}Cr_{0.04})(Si_{4.07}Al_{7.93})O_{40}$

Column 2: Rhönite, 3898; calculated formula $Ca_{3.95}(Mg_{5.85}Ti^{3}_{1.95}Ti^{4}_{1.95}Al_{1.03}V_{0.70}Fe_{0.61})(Si_{4.23}Al_{7.97})O_{40}$

Column 3: Fassaite, 3529-29; calculated formula $Ca_{0.97}(Mg_{0.32}Ti^{3}_{0.27}Ti^{4}_{0.27}Al_{0.11}V_{0.03})(Si_{1.16}Al_{0.84})O_6$

Column 4: Fassaite, 3898; calculated formula $Ca_{0.98}(Mg_{0.34}Ti^{3}_{0.27}Ti^{4}_{0.27}Al_{0.07}V_{0.03})(Si_{1.16}Al_{0.84})O_6$

has since been confirmed. Wark and Lovering (1980) have provided a detailed petrographic description of 3529-33, including the minute metal grains rich in Pt-group elements; this inclusion (identified as D1) was analyzed by Gray, Papanastassiou, and Wasserburg (1973), who showed that it had a very low $^{87}Sr/^{86}Sr$ ratio; Jessberger et al. (1980) have published K-Ar data. Material from 3898 (their D7) was analyzed by Gray, Papanastassiou, and Wasserburg (1973), who reported compositions of melilite and pyroxene, contents of Rb and Sr, and $^{87}Sr/^{86}Sr$ ratios; Rb is extremely low (0.01–0.02 ppm) and $^{87}Sr/^{86}Sr$ is the lowest yet measured, identifying this material as a very early condensate from the solar nebula. Niederer, Papanastassiou, and Wasserburg (1980) found Ti isotope anomalies, and Becker and Epstein (1981) consider it a FUN inclusion (inclusions showing isotopic fractionation (F) and unidentified nuclear (UN) effects), anomalous in ^{48}Ca, ^{18}O, and ^{17}O.

Group V

Group V inclusions were distinguished by Taylor and Mason (1978) on the basis of their RE distribution pattern, which is essentially unfractionated with no significant anomalies (Figure 8). Four such inclusions have been recognized, and their mineralogical compositions are given in Table 4. In major-element chemistry and in mineralogical composition and texture they are practically indistinguishable from Group I inclusions.

Table 4.—Mineralogical composition of Group V inclusions (estimated weight percentages of minerals; range and mean Ak content of melilite)

Inclusion	Melilite	Fassaite	Spinel	Anorthite	Ak range and mean
3529-21	30	40	20	10	17–47, 33
3529-45	70	20	10	0	4–15, 9
3655A	30	50	10	10	12–56, 24
3682	40	40	10	10	20–43, 26

Inclusion 3529-45 does have some unique features; it consists largely of Al-rich melilite (note the low Ak content given in Table 4), and the fassaite is associated with small areas of intergrown perovskite, spinel, and hibonite (Figure 9)—this mineral association is highly suggestive of decomposed rhönite. Minor and trace element concentrations (Table 1) are similar to those in Group I inclusions.

Steele and Hutcheon (1979) have published an Al-Mg isochron determined by ion microprobe on coexisting spinel, melilite, and hibonite in 3529-45. Herzog et al. (1980) have reported mineral compositions and ^{39}Ar–^{40}Ar systematics on 3655A.

Group III

Group III inclusions are characterized by an unfractionated RE distribution pattern at 10–40 times chondrites, except for negative Eu and

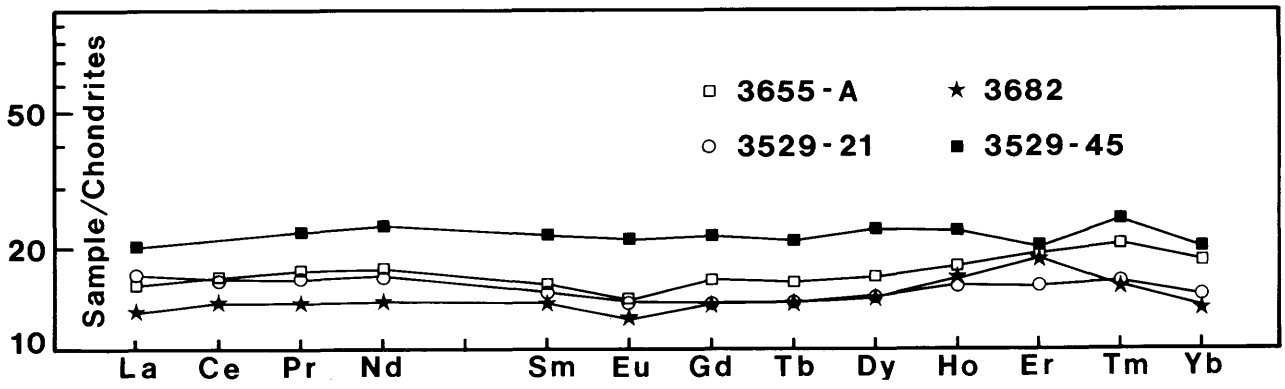

Figure 8.—RE distribution patterns for Group V Allende CAIs.

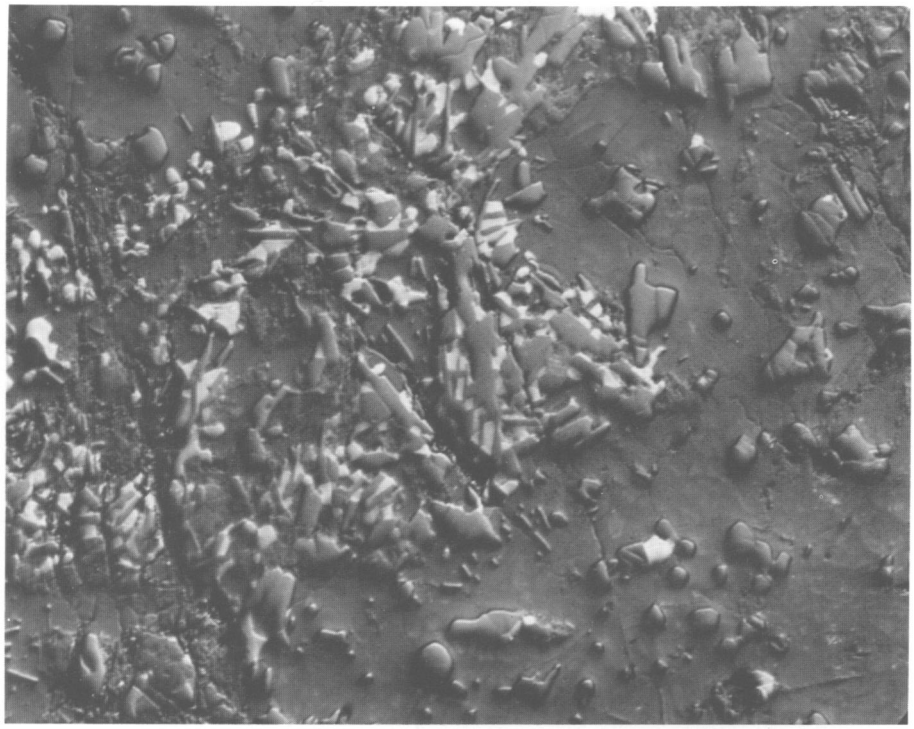

FIGURE 9.—Spinel (cubes)–hibonite (laths)–perovskite (white) intergrowth in Allende 3529-45 (reflected light); this association suggests an origin by the decomposition of rhönite.

Yb anomalies of equal magnitude (Figure 10). The first pattern of this kind was described by Tanaka and Masuda (1973); this was determined on a portion of 3529-O. Mason and Martin (1977) described two Group III inclusions (3593 and 4698). We have studied four Group III inclusions, and their mineralogical compositions are given in Table 5. In major-element composition they are similar to Group I inclusions, except for higher Al_2O_3 and lower CaO contents. Group III inclusions, however, show a variety of textural relationships, from coarse-grained chondrule-like objects to fine-grained irregular aggregates; some show complex internal rimming associated with the alteration of melilite to grossular (Figure 11). Inclusion 3529-42 has areas extremely rich in hibonite (Figure 12); inclusion 3529-46 has areas rich in perovskite, suggestive of the decomposition of rhönite (Figure 13).

TABLE 5.—Mineralogical composition of Group III inclusions (estimated weight percentages of minerals; range and mean Ak content of melilite)

Inclusion	Melilite	Fassaite	Spinel	Anorthite	Ak range and mean
3529-O	40	40	20	0	25–40, 35
3529-41	30	30	20	20	22–39, 30
3529-42	40	15	35	10	1–4, 3
3529-46	55	20	20	5	3–12, 6

Minor and trace element concentrations in Group III inclusions (Table 1) are generally similar to those in Group I inclusions (except for the Eu and Yb anomalies).

Lorin and Christophe Michel-Lévy (1978) have described metal grains, vanadium oxide inclusions, and Mg isotopic anomalies in 3529-42. Wark (1981a) has published analyses of nepheline, sodalite, anorthite, spinel, grossular, andradite, and pyroxene from 3593 and estimated its primary and altered composition.

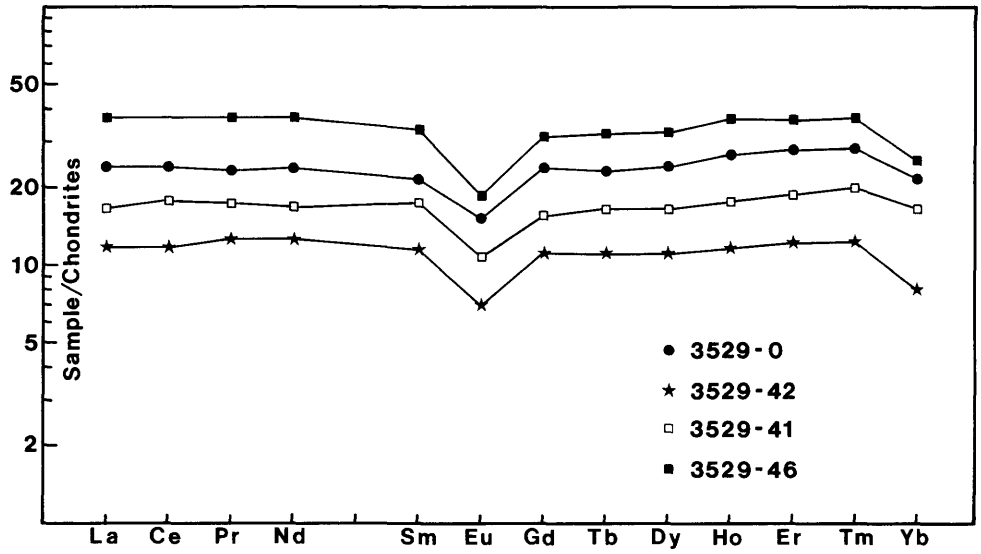

FIGURE 10.—RE distribution patterns for Group III Allende CAIs.

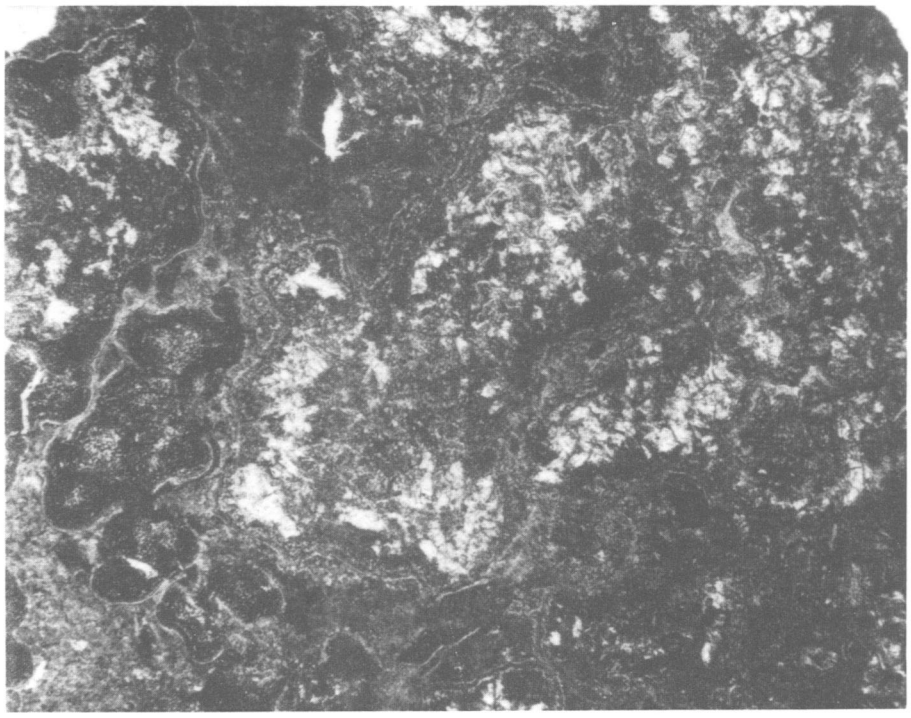

FIGURE 11.—Photomicrograph (transmitted light) of Allende 3529-46, a Group III CAI, consisting largely of melilite (white) and spinel, the melilite much altered to grossular (gray, fine-grained). Note extensive internal rims.

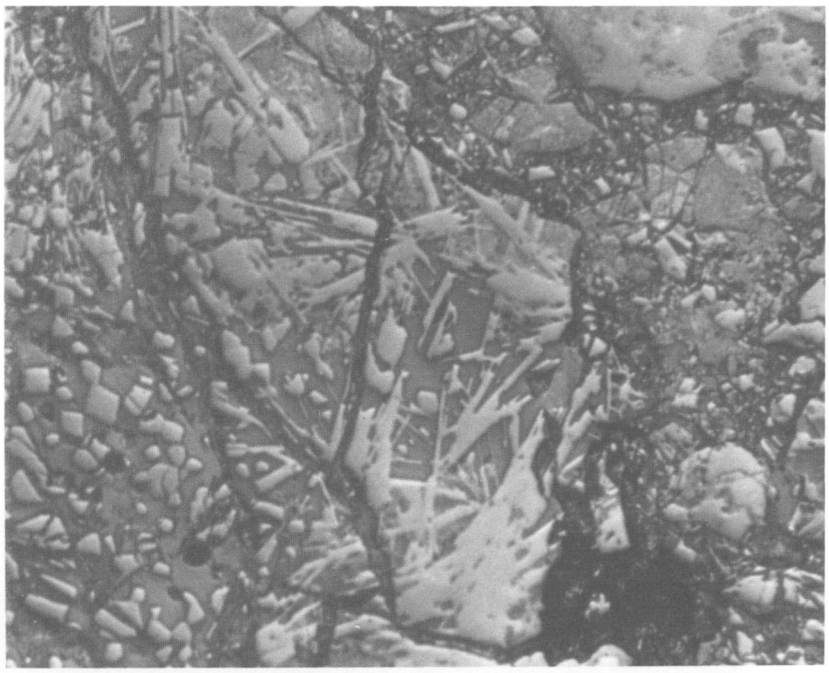

FIGURE 12.—Photomicrograph (reflected light) of a portion of Allende 3529-42, a Group II CAI, showing hibonite (laths) and spinel (cubes) in melilite.

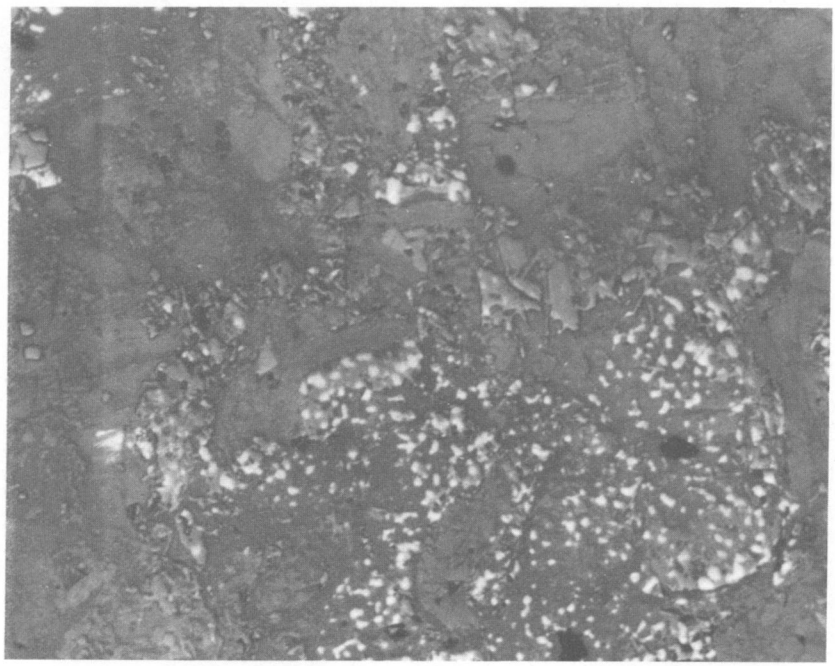

FIGURE 13.—Photomicrograph (reflected light) of a portion of Allende 3529-46, showing a concentration of perovskite (white, grains ~ 2–4 micrometers).

Group VI

Group VI inclusions were characterized by Taylor and Mason (1978) as having flat RE distribution patterns except for positive Eu and Yb anomalies (Figure 14). These patterns are complementary to those of Group III, although the Eu and Yb anomalies are not so pronounced in the Group VI inclusions. Inclusions 5171 and 3529-36, described in Mason and Martin (1977) as Group I and unclassified, should also be included in Group VI. Group VI inclusions show a wide range in chemical and mineralogical compositions and in textures. Inclusion 3529-Y is a melilite-rich chondrule, quite similar to the numerous Group I chondrules, as is inclusion 5171. Inclusion 3529-44 is an irregular medium-grained white inclusion (possibly a deformed chondrule)

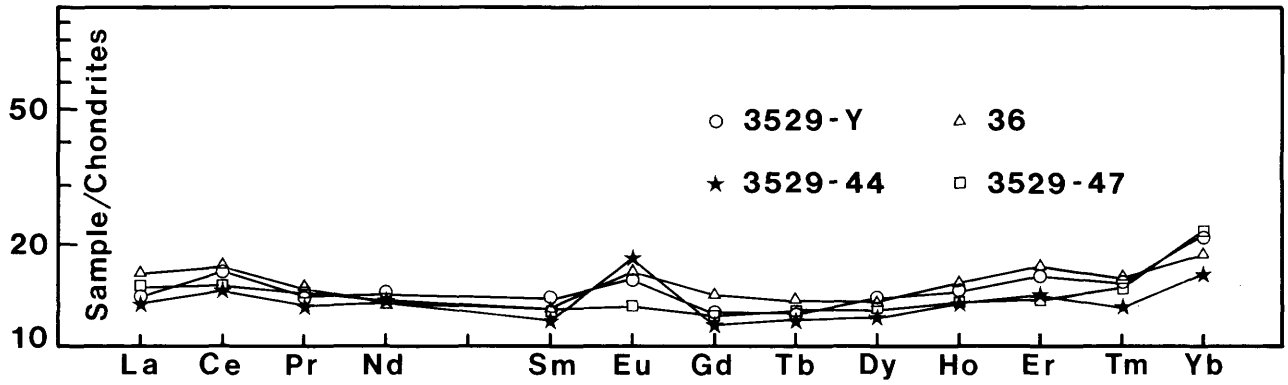

Figure 14.—RE distribution patterns for Group VI Allende CAIs.

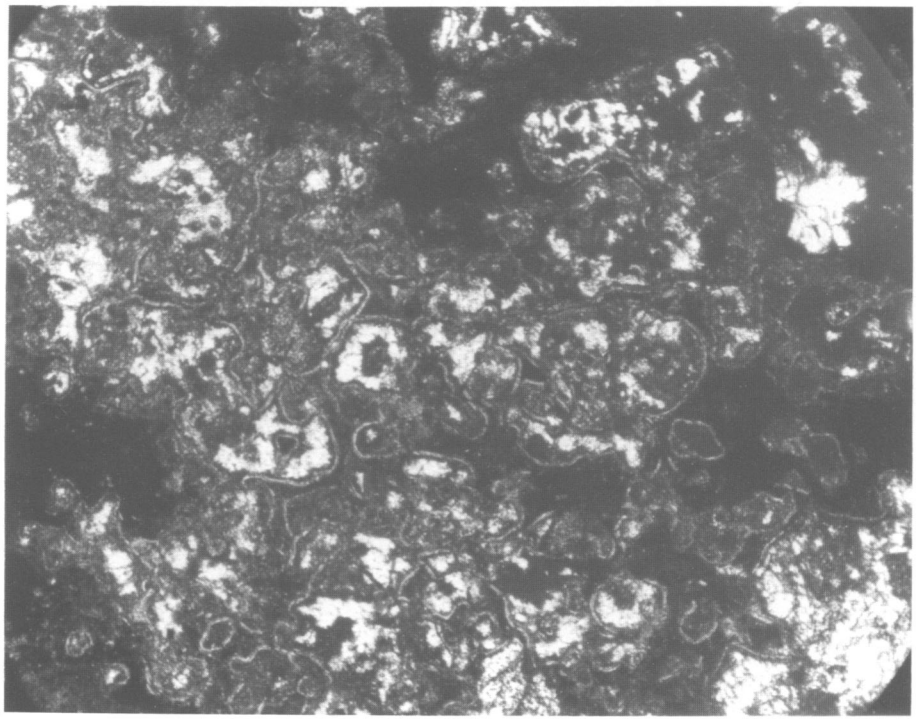

Figure 15.—Photomicrograph (transmitted light) of Allende 3529-47, a Group VI CAI, showing melilite (white) largely altered to grossular-andradite (gray, fine-grained) and rimmed by diopside.

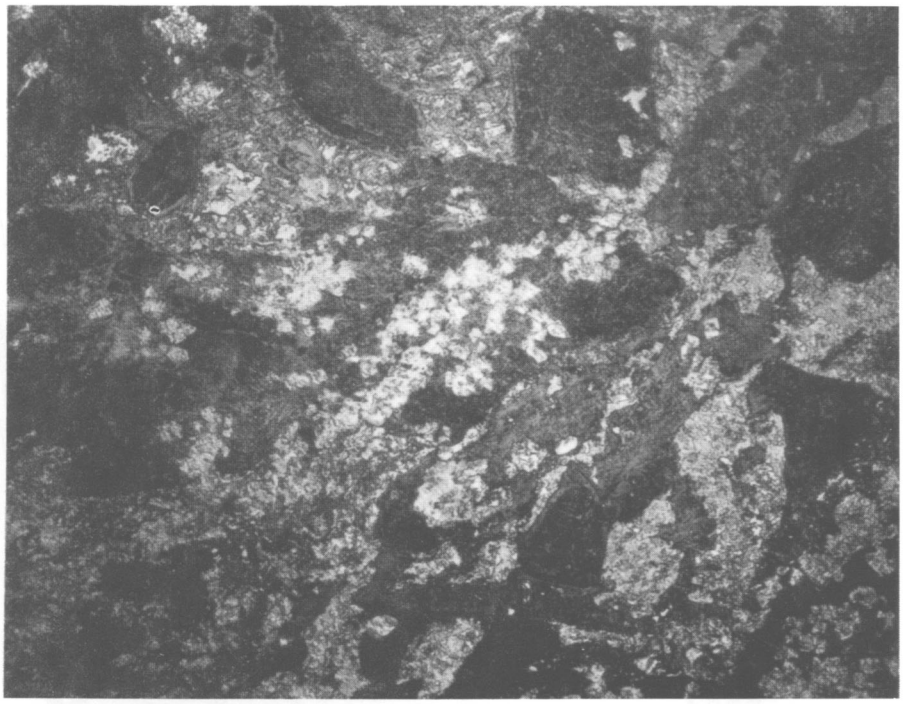

FIGURE 16.—Photomicrograph (transmitted light) of Allende 3529-36, a Group VI CAI, showing andradite (dark gray to black) with lighter areas of nepheline, sodalite, and melilite.

consisting largely of melilite (mean composition Ak_{27}) which is extensively altered to grossular. Inclusion 3529-47 is an unzoned aggregate, 15 mm in maximum dimension, consisting largely of gehlenitic melilite (mean composition Ak_3); the melilite is extensively altered to grossular or andradite and is rimmed by diopside (Figure 15). Inclusion 3529-36 is a large rounded aggregate, possibly a deformed and altered chondrule; it is unique in Allende inclusions so far examined in consisting largely of andradite (Figure 16), possibly pseudomorphous after melilite or fassaite. Except for the Eu and Yb anomalies, the trace-element concentrations in Group VI inclusions are similar to those in Group I inclusions.

Becker and Epstein (1981) have reported a ^{29}Si deficiency in 3529-Y.

GROUP II

Group II inclusions show a highly fractionated RE distribution pattern, characterized by the light RE (La-Sm) at 10–50 × chondrites, a negative Eu anomaly, a very rapid decline in relative abundances from Gd to Er, a strong positive Tm anomaly (Tm ≃ Sm), and Yb abundance comparable with that for Eu (Figure 17). This pattern was first recognized by Tanaka and Masuda (1973) in their Allende inclusion G (inclusion 3598 in Mason and Martin (1977)). Mason and Martin described five Group II inclusions, and we have found five more (Table 1).

All the Group II inclusions except one are fine-grained (average grain size 0.01–0.04 mm) irregular aggregates (Figure 18), white to pink (the pink color usually indicates a richness in spinel). The exception is 4691, a large irregular inclusion (maximum dimension 15 mm) consisting largely of melilite (Ak_{5-12}, average Ak_7) with abundant spinel inclusions, and a little fassaite and anorthite (Figure 19). Group II inclusions show a wide range in major-element composition (Table 1 and Figure 4); most of them show relatively high alkali and FeO contents (Na_2O up to 4.7%, FeO up to 13%). The wide range in major-element composition is reflected in a wide range in min-

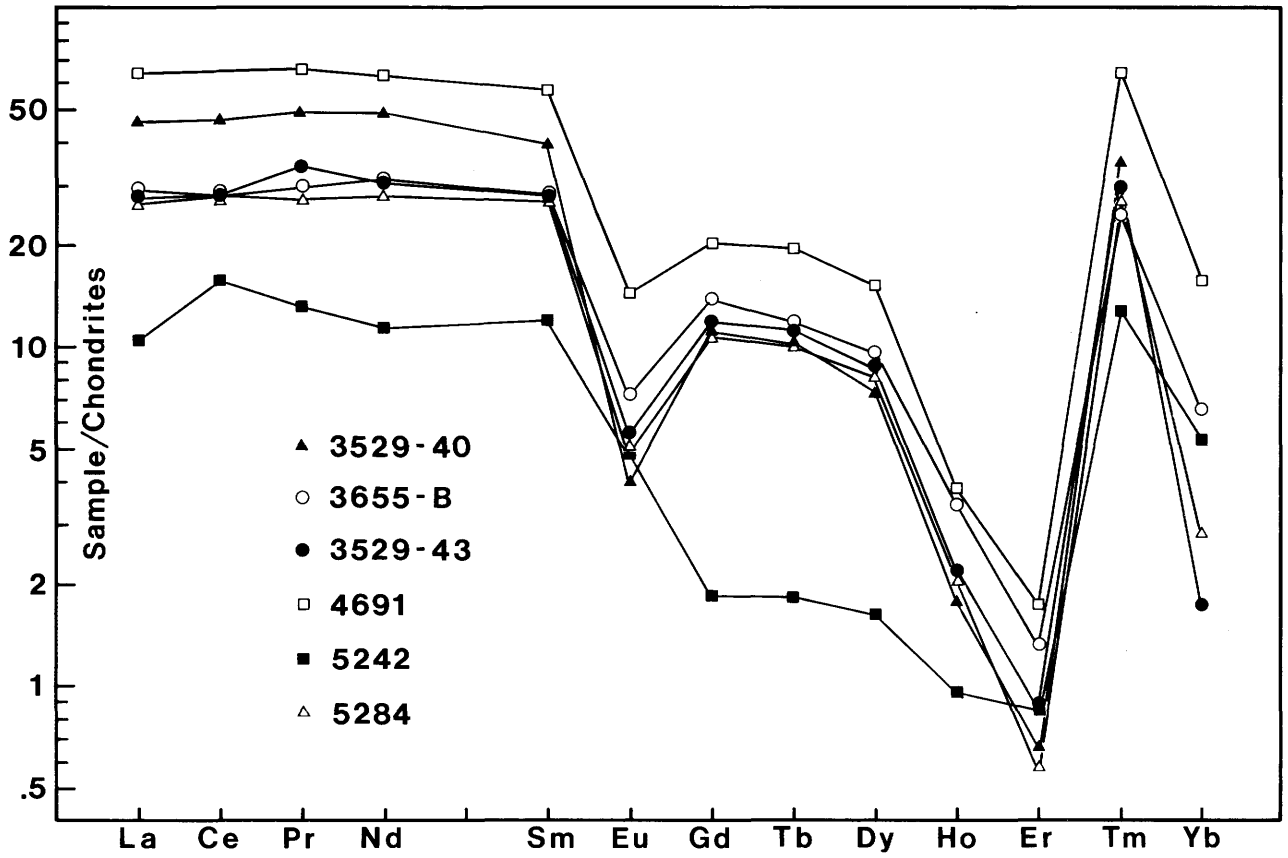

FIGURE 17(upper).—RE distribution patterns for Group II Allende CAIs.

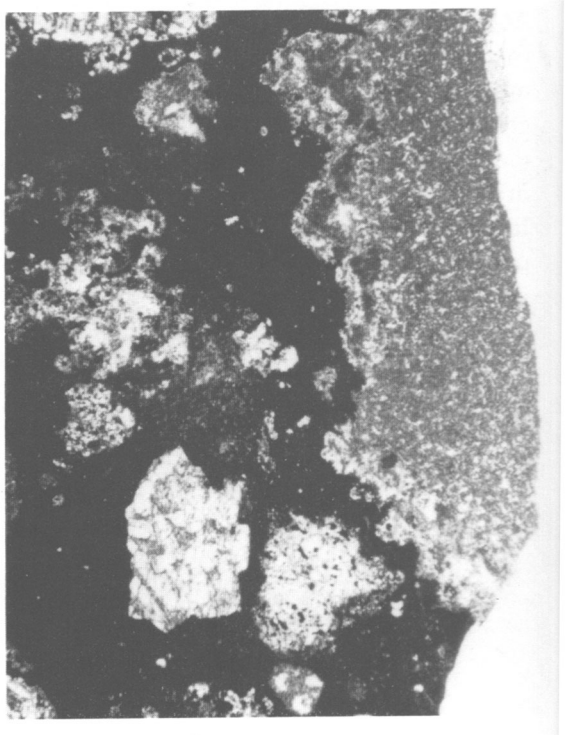

FIGURE 18(right).—Photomicrograph of Allende 3529-37, a fine-grained Group II CAI, consisting of fine-grained melilite, fassaite, and spinel, with some nepheline and sodalite; black material is fine-grained matrix.

eralogical composition. Modal composition cannot be precisely determined because of the fine-grained nature of these inclusions; microscopic examination, X-ray diffraction, and microprobe data show that the minerals include major melilite, fassaite, and spinel, minor nepheline and sodalite and possibly anorthite, and accessory perovskite and hibonite; grossular and grossular-andradite are usually present, possibly as alteration products of melilite. Figure 20 illustrates the texture of a typical fine-grained Group II inclusion, as revealed in the scanning electron microscope. It is markedly porous and consists of an aggregate of μm-sized anhedral mineral grains,

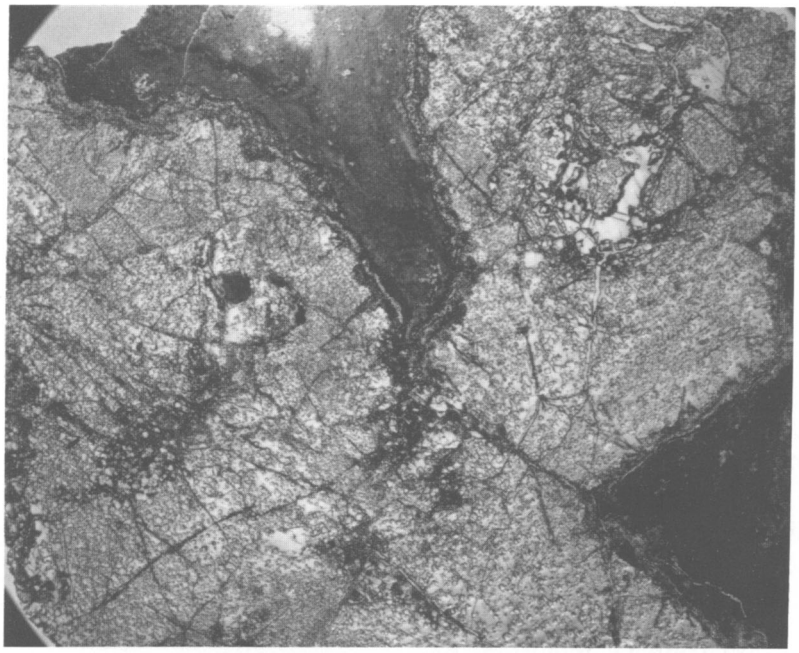

FIGURE 19.—Photomicrograph (transmitted light) of Allende 4691, a coarse-grained Group II CAI, consisting of melilite (white) enclosing innumerable micrometer-sized spinel grains; dark material is surrounding matrix.

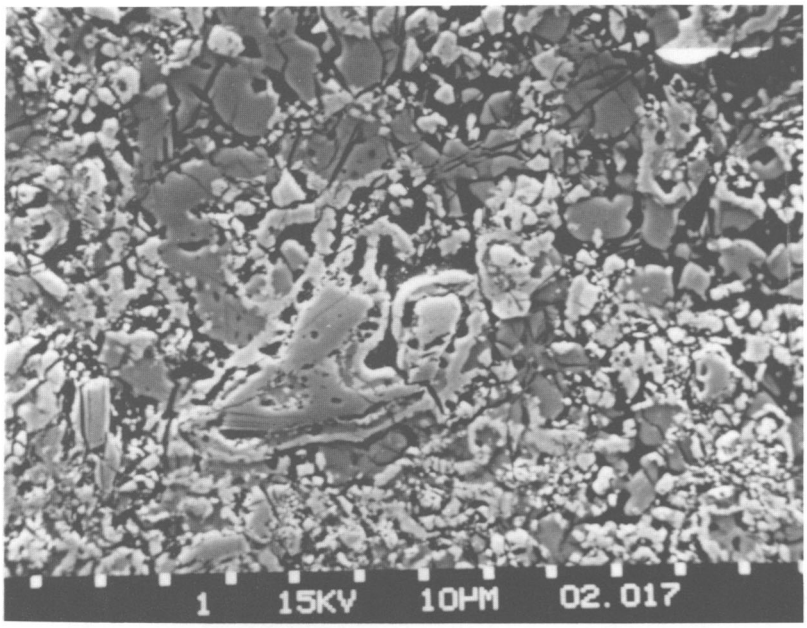

FIGURE 20.—Scanning electron micrograph of Allende 4692, a fine-grained Group II CAI; white is largely spinel and pyroxene, with some hibonite; gray is nepheline and sodalite, black is pore space.

sometimes aggregated into chains; the whole appearance is suggestive of a flocculated mass of dust particles.

As well as their characteristic RE patterns, Group II inclusions are distinctly different from other CAIs in other trace elements. They are relatively depleted in Y, Zr, Hf, Nb, and the platinum-group elements.

Niederer, Papanastassiou, and Wasserburg (1981) have published Ti isotopic data, and Chen and Wasserburg (1981) report on U-Pb isotopic compositions in 3529-40. For 4691 Wark (1981b) has estimated primary and altered compositions; Jessberger et al. (1980) have published K-Ar data; and Niemeyer and Lagmair (1980) have reported Ti isotopic compositions.

Group IV

We have no data on Group IV inclusions beyond those published by Mason and Martin (1977). As mentioned previously, these olivine-rich inclusions are relatively low in Ca and Al and on that account should perhaps be excluded from the CAIs.

Platinum-Group Elements

(Data from Table 1 only)

Although the RE have proven most useful in distinguishing among the various classes of Allende inclusions, other trace elements show some characteristic differences. The Group II inclusions contain abundances of Ru, Rh, Pd, Os, Ir, and Pt at about chondritic levels (our analytical technique was not sensitive enough to detect Re at this level).

In contrast, Groups I, III, V, and VI are enriched in the refractory trace elements Ru, Re, Os, Ir, and Pt at 10–20 times chrondritic levels. They show a relative depletion in Rh (5 × Cl abundances) and particularly in Pd (2–3 × Cl abundances) (Figure 21). There is a good correlation between the relative abundances and the condensation temperatures for these elements in Groups I, III, V, and VI (Figure 22). Thus the element fractionations are clearly linked to relative volatility. It is curious that the Group II inclusions show about chondritic levels of the Pt-group elements, despite the evidence of extreme fractionation evident in the RE patterns.

Th/U Ratios

(Data from Table 1 only)

The analytical data for these elements are both precise and accurate by the SSMS technique. Wide variations among the ratios are found among the inclusions (Table 1). Only in Group VI is the ratio chondritic (3.8) or below. Groups I, III, and V have ratios ranging from 4.7–13 with little overlap between the groups. One Group II inclusion (5242) has a chondritic ratio, but the others show values up to 24.3. This variation is attributed mainly to changes in the abundance levels of uranium relative to the more refractory element thorium.

La/Th Ratios

(Data from Table 1 only)

Thorium appears to behave in a very similar manner to the light RE, La, in Groups I, III, V, and VI. The La/Th ratio is 8.50 ± 1.45, which is essentially equivalent to the chondritic ratio of 8.51. The correlation coefficient (r) for 12 samples is 0.963, illustrating that there is no fractionation between these elements. In contrast, the Group II inclusions (6 samples) have La/Th = 13.50 ± 1.5, with a correlation coefficient of 0.969. In these inclusions La is thus enriched uniformly over Th by a factor of 1.6.

Zr-Hf-Y-Er

(Data from Table 1 only)

The extreme behavior of Er in the Group II inclusions makes it of interest to identify other

FIGURE 21(upper).—Platinum-group element distribution patterns in Allende CAIs.

FIGURE 22(lower).—Correlation between relative abundances and condensation temperatures for platinum-group elements in Allende CAIs.

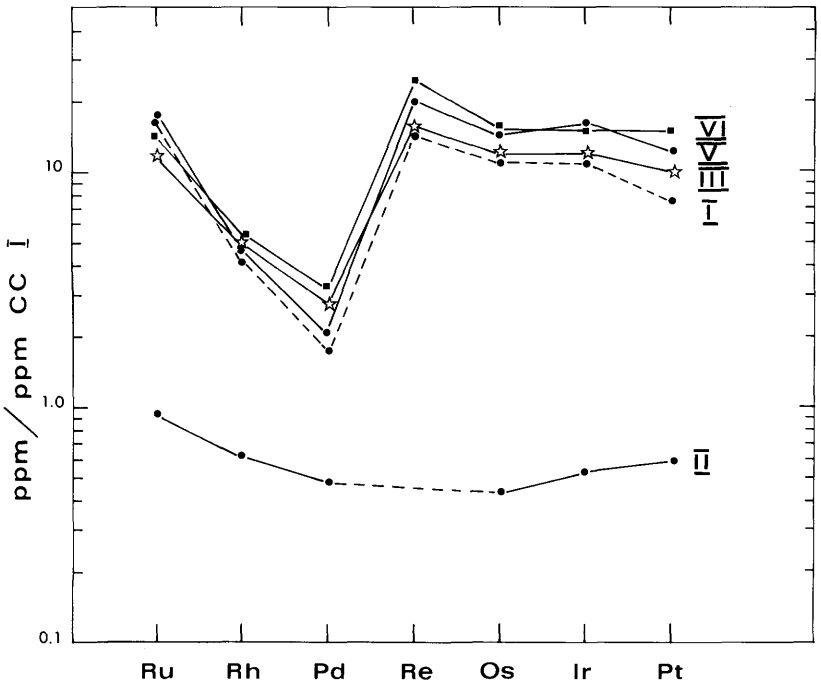
ppm / ppm CC I
10
1.0
0.1
VI
V
III
I
II
Ru
Rh
Pd
Re
Os
Ir
Pt

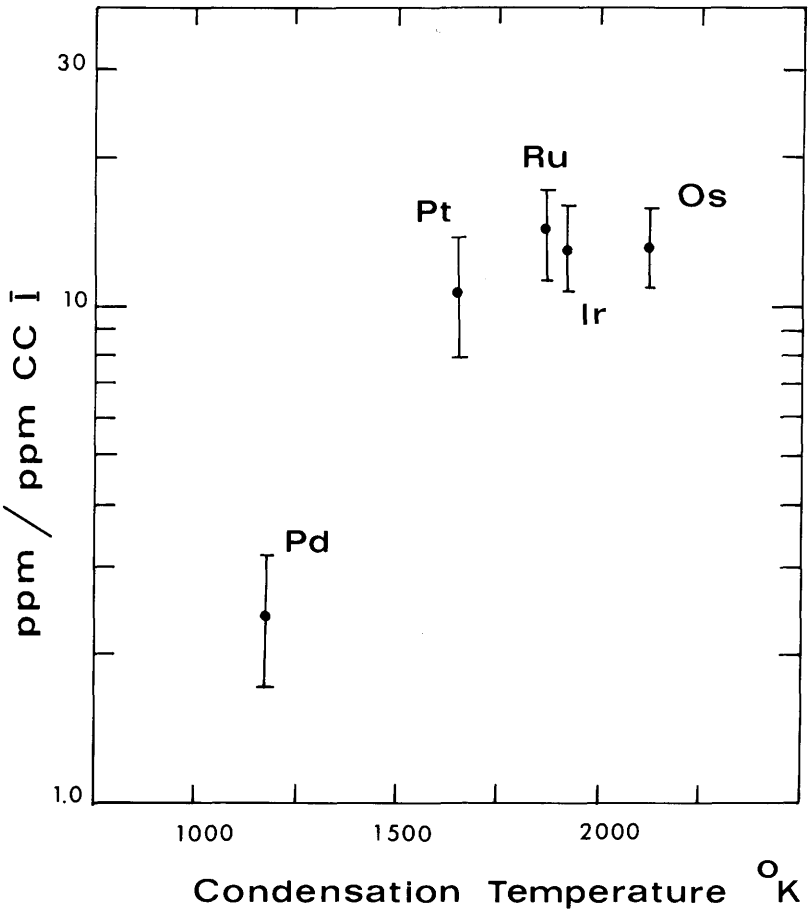
ppm / ppm CC I
30
10
1.0
Ru
Pt
Os
Ir
Pd
1000
1500
2000
Condensation Temperature °K

elements showing similar characteristics. The parallel behavior of Y to the heavy RE in many geochemical processes also makes it useful to compare its distribution in the Allende inclusions. In Groups I, III, V, and VI, Y correlates with the heavy RE, since they have patterns parallel to those of chondrites. In Group II, Y correlates with Er but not with neighboring Ho or Tm. Accordingly, Y and Er must have similar volatilities. The Y/Er ratio is constant at 9.4 ± 1.8 for all inclusions. The correlation coefficient r=0.945 for 18 samples. The chondritic ratio for Y/Er is 9.39, and, accordingly, yttrium and erbium show a closely coherent relationship during cosmochemical processes.

Other elements which show a close correlation with Y and Er are Zr and Hf. Zr/Y is constant for all inclusions at 2.34 ± 0.30. Our Zr data by SSMS are less precise than those for Hf, but the Zr/Hf ratio is 36 ± 4.9 for all inclusions. This value is not distinguishable from the chondritic ratio of 33, the difference being due to the less precise nature of our Zr values. Accordingly, these four elements must have similar volatility characteristics and remain locked together in cosmochemical processes.

Unclassified CAIs

We have found some CAIs, and others have been described in the literature, that appear to be different from any of those described above. Unfortunately, for most of them no RE data are available.

Inclusion 3509 is a chalky-white chondrule, 8 mm in diameter (Figure 23). It was found in one of the first Allende specimens collected and was described by Clarke et al. (1970:39), as follows:

> A single chondrule of type *c* has been found. It was observed on a broken fragment of the meteorite, being unusually large (8 mm in diameter) and a uniform chalky-white color. It is so fine-grained that the individual minerals could not be identified in grain mounts in immersion oils. X-ray powder photographs provided positive identification for sodalite, nepheline, clinopyroxene (probably fassaite), and olivine, and this mineralogy is consistent with the bulk chemical composition of the chondrule (Table 3, column 8). By the X-ray procedure of Yoder and Sahama (1957) the composition of the olivine was found to be Fa_{26}, in good agreement with the FeO/(FeO+MgO) ratio in the chemical analysis. This occurrence of sodalite ($Na_8Al_6Si_6O_{24}Cl_2$, with 7.3 percent Cl), the first recorded from a meteorite, is particularly intriguing, since the chlorine content of stony meteorites is usually low (of the order of 100 ppm) and combined as chlorapatite. Microprobe analyses have confirmed the presence of nepheline and sodalite, and have provided some significant compositional data; in particular, potassium is notably fractionated between the two minerals, the nepheline containing 1.5 percent K and the sodalite less than 0.1 percent. The extremely fine-grained texture of this chondrule suggests that it solidified as a glass and subsequently devitrified.

Grossman and Steele (1976:150) commented that "Clarke et al. (1970) gave a very accurate description of an amoeboid aggregate but they classified it as a type *c* Ca-Al-rich *chondrule*" [their italics]. Since they never saw the specimen, their reclassification of it as an amoeboid aggregate is evidently based on their interpretation of the above description; however, this inclusion is certainly not amoeboid.

The phase composition, estimated from the chemical analysis and the minerals present, is (weight percent): olivine (Fa_{26}) 35, nepheline 30, sodalite 20, pyroxene 15. Mason and Martin (1977) determined minor and trace elements; the RE concentrations are low (at about average chondritic abundances, but with a positive Eu anomaly (Eu/Eu* = 2.9). This inclusion does not fall in any of the previously described RE groups.

Wasserburg and Huneke (1979) have shown that this inclusion is extremely enriched in ^{129}Xe evidently produced from ^{129}I, presumably incorporated in the halogen-rich mineral sodalite.

Unfortunately, despite many searches through large collections of Allende material, no further specimens of this unique chondrule type have been found.

Inclusion 3510 has been observed only in thin section, so no chemical data are available except for microprobe analyses of the individual minerals. It is a chondrule, 2.4 mm across (Figure 24),

FIGURE 23.—Allende 3509: *a*, chondrule, 8 mm in diameter, in matrix; *b*, scanning electron microphotograph showing olivine (light gray, radiating), sodalite (black, interstitial), and diopside (light gray, blocky, at lower left).

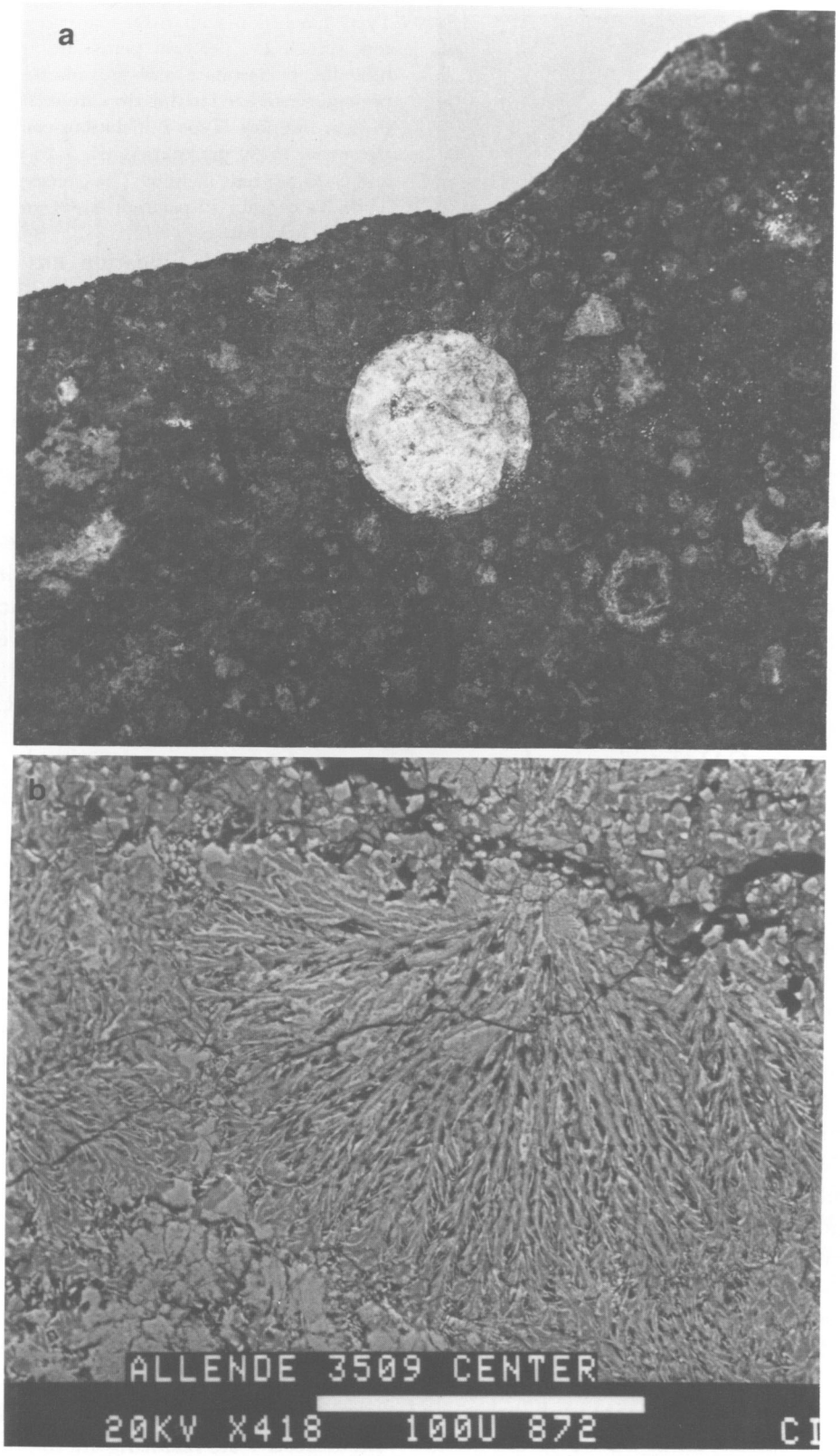
a
b
ALLENDE 3509 CENTER
20KV X418 100U 872

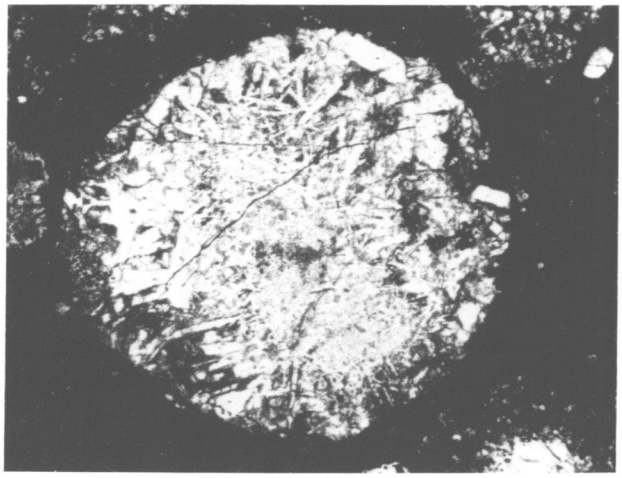

FIGURE 24.—Photomicrograph (transmitted light) of anorthite-fosterite-spinel chondrule (2.4 mm across) in Allende 3510.

consisting of anorthite, An_{96} (80%), forsterite, Fa_1 (15%), and spinel (5%). From the composition of the minerals and the mode, the bulk composition (weight percent) is SiO_2, 40.3; Al_2O_3, 32.7; FeO, 0.2; MgO, 10.4; CaO, 16.1; Na_2O, 0.3, which clearly puts it in the CAI classification.

Fuchs (1969) described an irregular inclusion, 1.0 × 0.7 mm, consisting of cordierite with aluminous enstatite, anorthite, spinel, olivine, and sodalite. This is the first, and so far the only, record of cordierite in a meteorite. Repeated searches through a large collection of Allende specimens have failed to find another specimen. Cordierite, anorthite, and spinel are liquidus phases in the 10% MgO plane which approximates the composition of many Allende CAIs, and this inclusion may represent a slightly more SiO_2-rich composition than other CAIs.

Several CAIs with apparently unique mineralogical compositions have been mentioned in the literature, and investigations of their RE distribution patterns may reveal additional groupings.

Discussion

Grossman (1975:443) proposed a classification of coarse-grained Allende CAIs into two types, as follows:

Type A inclusions contain 80–85 per cent melilite, 15–20 per cent spinel, 1–2 per cent perovskite and rare plagioclase, hibonite, wollastonite and grossularite. Clinopyroxene, if present, is restricted to thin rims around inclusions or cavities in their interiors. Type B inclusions contain 35–60 per cent pyroxene, 15–30 per cent spinel, 5–25 per cent plagioclase and 5–20 per cent melilite. The coarse pyroxene crystals in Type B's contain 15 per cent Al_2O_3 and 1.8% Ti, some of which is trivalent.

Grossman's classification has been widely, if somewhat uncritically, accepted by researchers on Allende CAIs; however, it is extremely restrictive in its compositional limits, as is shown in Figure 25. The requirement that Type A inclusions contain at least 80% melilite means that CaO in the bulk composition must be 32% or greater (since melilite contains 40%–41% CaO). We have plotted on Figure 25 the estimated mineral composition of our coarse-grained CAIs, none of which falls within the limits set by Grossman for his Type A and Type B inclusions. Either his classification is too restrictive, or it is not applicable to the coarse-grained inclusions we have studied. Unfortunately his RE data (Grossman and Ganapathy, 1976) are inadequate to correlate his Type A–Type B classification with the RE groups defined in this paper.

Since the first descriptions of CAIs in the Allende meteorite there have been lively discussions as to their genesis. Marvin, Wood, and Dickey (1970) described several CAIs and suggested that they represented early, high-temperature condensates from the solar nebula; they noted the similarity between the chemistry and mineralogy of the CAIs and the sequence of compounds calculated by Lord (1965) to be among the highest temperature condensates to form in a solar nebula. This suggestion has been adopted and elaborated by several researchers, most notably by Grossman (1973, 1980), who concluded (1980: 584) that "the trace element results are thus very powerful evidence that coarse-grained inclusions formed in a gas-condensed phase fractionation process." Other experts, e.g., Kurat (1970), have concluded that CAIs are residues of an evaporation process, whereby more volatile components have been lost, resulting in the observed enrich-

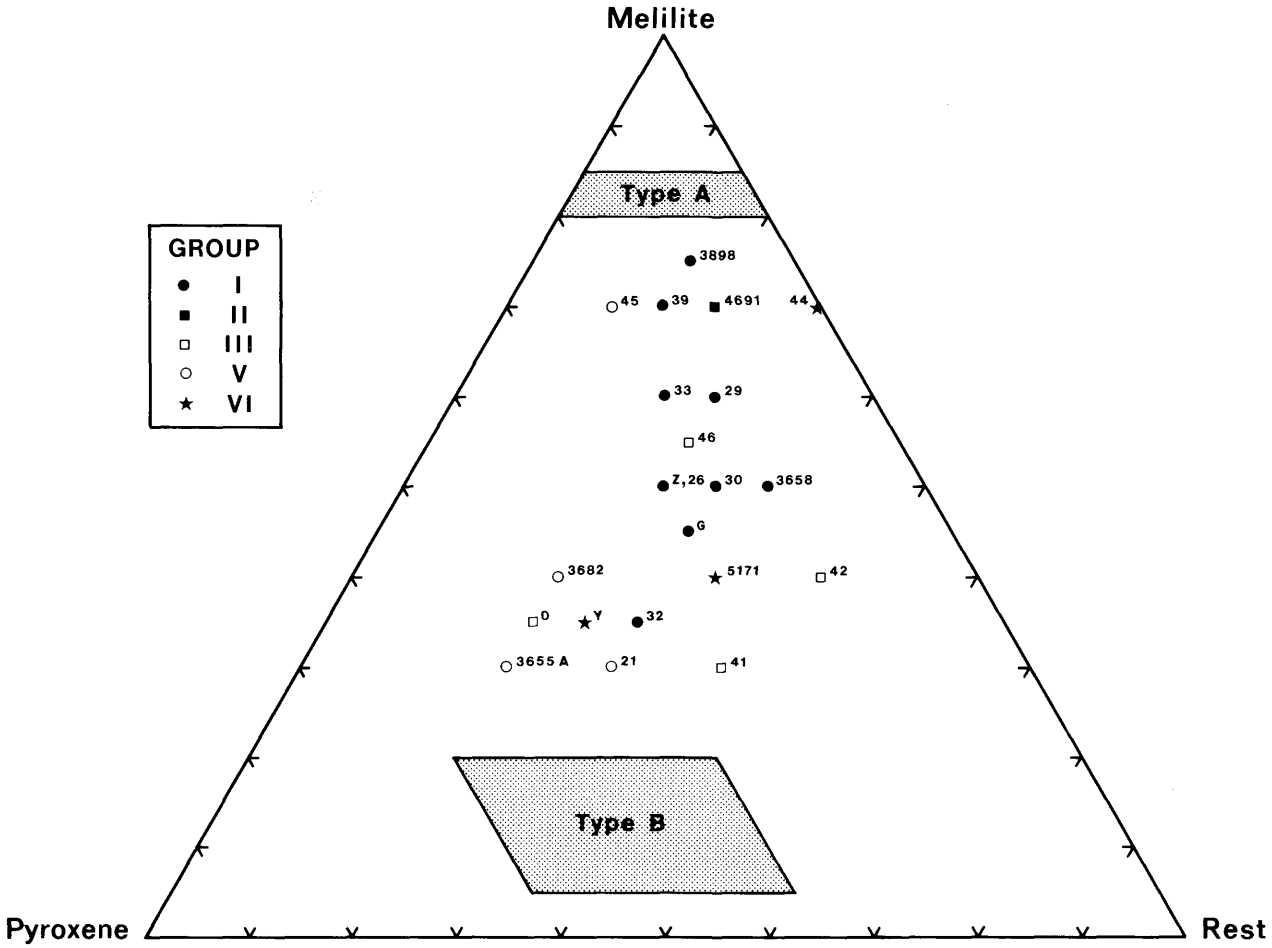

FIGURE 25.—Mineralogical composition of coarse-grained Allende CAIs and the compositional limits of Type A and B Allende inclusions as defined by Grossman (1975).

ment in the refractory elements. This process has been elaborated by Kurat, Hoinkes, and Fredricksson (1976) and by Chou, Baedecker, and Wasson (1976).

The variety and complexity of the Allende CAIs, and particularly the existence of distinct groups characterized by unique RE distribution patterns, indicate a complex origin. It is likely that their genesis was equally complex, and that neither fractional condensation nor fractional evaporation is the complete answer.

The Group I inclusions comprise a highly coherent group, very uniform in chemical and mineralogical composition. They are all coarse-grained melilite-rich chondrules, and the texture and crystallization sequence of the primary minerals strongly supports an origin as liquid silicate droplets. The major elements—Si, Al, Mg, Ca, Ti—are those predicted to condense at high temperatures in a cooling solar nebula (or to be residual in a fractional evaporation sequence). The small amounts of Fe and Na shown in bulk analyses of Group I inclusions were probably introduced in a gas phase after the inclusions had solidified; in all of them the melilite is partly altered along grain boundaries to a fine-grained material consisting largely of grossular, often with some nepheline. Group I inclusions show a uniform enrichment in RE and other refractory trace elements at 10–20 times chondritic abundances

and a small positive Eu anomaly, probably linked to the affinity of the element for the melilite structure. The minimum $^{87}Sr/^{86}Sr$ ratios recorded in some of them is additional evidence for their early formation, yet it is difficult to equate them with direct condensates from a cooling solar nebula. Most experts (e.g., Grossman, 1972) believe that such condensation must be gas-solid, not gas-liquid (although Blander and Katz (1967) have argued for nonequilibrium condensation in the form of supercooled liquid droplets). Gas-solid condensation would produce a dust of refractory solids, which must then be segregated from the cooling nebula and melted to give the chondrules. In this connection the giant size (up to 25 mm diameter) of the melilite-rich chondrules, in comparison to the common olivine-rich chondrules (average 1 mm diameter), may be significant. It indicates that some minimum amount of refractory-rich condensate had to accumulate before melting took place and suggests that some special factor may have been involved—an internal heat source such as postulated by Clayton (1980).

Group V inclusions are very similar to Group I inclusions in major and trace elements, and in mineralogy, but lack the positive Eu anomaly. They are melilite-rich chondrules, indistinguishable from Group I chondrules, except for 3529-45, which is a nonspherical melilite-rich inclusion, possibly a deformed chondrule.

Group III inclusions are more diverse in texture and composition, but all show characteristic negative Eu and Yb anomalies superimposed on a flat RE distribution pattern at 10–40 times chondritic abundances. This pattern is understandable in terms of the relatively volatility of the RE elements; Eu and Yb are the most volatile of these elements, and the observed pattern could be the result either of fractional condensation or fractional evaporation. The Group III inclusions comprise both coarse-grained (3529-O, 3529-41, 3529-42, 3529-46) and fine-grained (3593, 4698) types; the fine-grained inclusions are notably richer in alkalies (Na_2O, 1.3%–1.8%) than the coarse-grained inclusions (Na_2O, 0.21%–0.46%). Possibly the coarse-grained inclusions were formed from fine-grained precursors by heating and the loss of alkalies, without affecting the distribution of the more refractory elements.

Group VI inclusions show RE distribution patterns essentially complementary to those for Group III inclusions, i.e., undifferentiated except for small positive Eu and Yb anomalies (the Eu and Yb anomalies are not so pronounced as those in the Group III inclusions). Group VI inclusions are more varied in texture and mineralogy than other groups; inclusions 3529-Y, 5171, and probably 3529-44 are coarse-grained melilite-rich chondrules, whereas 3529-36 and 3529-47 are fine-grained aggregates. These inclusions range widely in major-element compositions; the melilite-rich chondrules are low in FeO, whereas the fine-grained aggregates are high in this component. The texture of 3529-36 suggests that it is a metasomatically altered melilite-rich chondrule, whereby the melilite and fassaite have been altered to an aggregate of nepheline, sodalite, and andradite; this alteration has not affected the concentration of minor and trace elements (except Ba, which is anomalously low).

Group II inclusions present the most intriguing problems of all the Allende CAIs. They are all fine-grained aggregates (except 4691) and show a wide range in major-element compositions. Nevertheless, the RE distribution patterns are unique and remarkably uniform, except for 5242, which has considerable lower RE concentrations than the others (Figure 17). Inclusion 4691 is unique among Group II inclusions in several respects. It is the only coarse-grained such inclusion; its major-element composition is distinctive in having the highest CaO and TiO_2 and the lowest SiO_2, FeO, MgO, and Na_2O contents; and it has the highest RE concentrations. All these features strongly suggest that 4691 may be a Group II inclusion that has experienced a high degree of fractional evaporation, whereby more volatile elements have been lost with the production of a refractory residue, consisting largely of melilite and spinel (note that the melilite is almost pure $Ca_2Al_2SiO_7$, the refractory end of the melilite series).

Boynton (1975, 1977) has provided an extensive discussion of the significance of the Group II

RE distribution. He concluded (1977:184) that

> The strong depletion of most of the heavier RE and the peculiar Eu, Yb, and Tm anomalies are all related to the volatility of the RE and are readily understood in terms of an equilibrium gas-solid fractionation. Because the Group II RE pattern requires a gas/solid fractionation and because it is depleted in the most refractory RE, these aggregates must indeed be condensates since refractory residues would be expected to be enriched in the most refractory RE.

He has since found the complementary RE pattern in a CAI from the Murchison meteorite (Boynton, Frazier, and Macdougall, 1980).

Wood (1981) has recently presented a scenario for the origin and early evolution of the solar system which is based to a large extent on his interpretation of the significance of the CAIs in the Allende meteorite. He considers that the CAIs are unlikely to be condensates but are distillation residues, and that therefore the depletion of super-refractory elements in Group II CAIs cannot have been accomplished by fractional condensation in the solar nebula. He concludes that this depletion, and presumably a number of other properties of the components of primitive meteoritic material, must be relics of pre-solar-system fractionations among different populations of interstellar dust grains.

Literature Cited

Ahrens, L.H., and H. von Michaelis
1969. The Composition of Stony Meteorites, III: Some Inter-Element Relationships. *Earth and Planetary Science Letters*, 5:395–400.

Becker, R.H., and S. Epstein
1981. Silicon and Oxygen Isotopes in Some Selected Allende Inclusions. In *Lunar and Planetary Science, XII*, pages 56–58. Houston: Lunar and Planetary Institute.

Blander, M., and J.L. Katz
1967. Condensation of Primordial Dust. *Geochimica et Cosmochimica Acta*, 31:1025–1034.

Boivin, P.
1980. Données expérimentales préliminaires sur la stabilité de la rhönite à l'atmosphère. *Bulletin de Minéralogie*, 103:491–502.

Boynton, W.V.
1975. Fractionation in the Solar Nebula: Condensation of Yttrium and the Rare Earth Elements. *Geochimica et Cosmochimica Acta*, 39:569–584.
1977. A Brief Review of the Chemistry of Ca,Al-rich Inclusions in the Allende Meteorite. *Meteoritics*, 12:183, 184.

Boynton, W.V., R.M. Frazier, and J.D. Macdougall
1980. Trace Element Abundances in Ultra-refractory Condensates from the Murchison Meteorite. *Meteoritics*, 15:269.

Chen, J.H., and G.J. Wasserburg
1981. The Isotopic Composition of Uranium and Lead in Allende Inclusions and Meteoritic Phosphates. *Earth and Planetary Science Letters*, 52:1–15.

Chou, C-L., P.A. Baedecker, and J.T. Wasson.
1976. Allende Inclusions: Volatile-Element Distribution and Evidence for Incomplete Volatilization of Presolar Solids. *Geochimica et Cosmochimica Acta*, 40:85–94.

Christophe Michel-Lévy, M.
1968. Un chondre exceptionel dans la météorite de Vigarano. *Bulletin de la Société Francaise de Minéralogie et de Cristallographie*, 91:212–214.

Clarke, R.S., Jr., E. Jarosewich, B. Mason, J. Nelen, M. Gomez, and J.R. Hyde
1970. The Allende, Mexico, Meteorite Shower. *Smithsonian Contributions to the Earth Sciences*, 5: 53 pages.

Clayton, D.D.
1980. Chemical Energy in Cold-Cloud Aggregates: The Origin of Meteoritic Chondrules. *Astrophysical Journal*, 239:L37–L41.

Clayton, R.N., L. Grossman, and T.K. Mayeda
1973. A Component of Primitive Nuclear Composition in Carbonaceous Meteorites. *Science*, 182:485–488.

Dowty, E., and J.R. Clark
1973. Crystal Structure Refinement and Optical Properties of a Ti^{3+} Fassaite from the Allende Meteorite. *American Mineralogist*, 58:230–242.

El Goresy, A., K. Nagel, and P. Ramdohr
1977. Type A Ca,Al-rich Inclusions in Allende Meteorite: Origin of the Perovskite-Fassaite Symplectite around Rhönite and Chemistry and Assemblages of the Refractory Metals (Mo, W) and Platinum Metals (Ru, Os, Ir, Re, Rh, Pt). *Meteoritics*, 12:216.

El Goresy, A., K. Nagel, B. Dominik, P. Ramdohr, and B. Mason
1979. Ru-bearing Phosphate-Molybdates and Other Oxidized Phases in Fremdlinge in Allende Inclusions. *Meteoritics*, 14:390, 391.

El Goresy, A., and P. Ramdohr
1980. Osmium Depletion in Fremdlinge in an Allende Inclusion: Possible Supernova Material. In *Lunar and Planetary Science, XI*, pages 257, 258. Houston: Lunar and Planetary Institute.

Fruland, R.M., E.A. King, and D.S. McKay
1978. Allende Dark Inclusions. In *Proceedings of the Ninth Lunar and Planetary Science Conference*, pages 1305–1329. New York: Pergamon Press.

Fuchs, L.H.
1969. Occurrence of Cordierite and Aluminous Orthoenstatite in the Allende Meteorite. *American Mineralogist*, 54:1645–1653.
1978. The Mineralogy of a Rhönite-bearing Calcium Aluminum Rich Inclusion in the Allende Meteorite. *Meteoritics*, 13:73–78.

Gast, P.W., N.J. Hubbard, and H. Wiesmann
1970. Chemical Composition and Petrogenesis of Basalts from Tranquility Base. In *Proceedings of the Apollo 11 Lunar Science Conference*, pages 1143–1163. New York: Pergamon Press.

Gray, C.M., D. A. Papanastassiou, and G.J. Wasserburg
1973. The Identification of Early Condensates from the Solar Nebula. *Icarus*, 20:213–239.

Grossman, L.
1972. Condensation in the Primitive Solar Nebula. *Geochimica et Cosmochimica Acta*, 36:597–619.

1973. Refractory Trace Elements in Ca-Al-rich Inclusions in the Allende Meteorite. *Geochimica et Cosmochimica Acta*, 37:1119–1140.
1975. Petrography and Mineral Chemistry of Ca-rich Inclusions in the Allende Meteorite. *Geochimica et Cosmochimica Acta*, 39:433–454.
1980. Refractory Inclusions in the Allende Meteorite. *Annual Review of Earth and Planetary Sciences*, 8:559–608.

Grossman, L., and R. Ganapathy
1976. Trace Elements in the Allende Meteorite, I: Coarse-grained, Ca-rich Inclusions. *Geochimica et Cosmochimica Acta*, 40:331–344.

Grossman, L., and I.M. Steele
1976. Amoeboid Olivine Aggregates in the Allende Meteorite. *Geochimica et Cosmochimica Acta*, 40:149–155.

Haggerty, S.E.
1977. Refinement of the Ti-Cosmothermometer in the Allende Meteorite and the Significance of a New Mineral, $R^{2+}Ti_3O_7$, in Association with Armalcolite. In *Lunar Science, VIII*, pages 389–391. Houston: Lunar Science Institute.

Herzog, G.F., A.E. Bence, J.F. Bender, G. Eichhorn, H. Maluski, and O.A. Schaeffer
1980. ^{39}Ar–^{40}Ar Systematics of Allende Inclusions. In *Proceedings of the Eleventh Lunar and Planetary Science Conference*, pages 959–976. New York: Pergamon Press.

Jessberger, E.K., B. Dominik, T. Staudacher, and G.F. Herzog
1980. ^{40}Ar–^{39}Ar Ages of Allende. *Icarus*, 42:380–405.

Jordan, J., E.K. Jessberger, T. Kirsten, and A. El Goresy
1980. Alien Xenon in Allende Inclusions. *Meteoritics*, 15:309, 310.

Kornacki, A.S.
1981. Are CAI's Condensates of Distillation Residues? Evidence from a Comprehensive Study of Fine- to Medium-grained Inclusions in the Allende C3(V) Carbonaceous Chondrite. In *Lunar and Planetary Science, XII*, pages 562–564. Houston: Lunar and Planetary Institute.

Kurat, G.
1970. Zur Genese der Ca-Al-reichen Einschlüsse im Chondriten von Lancé. *Earth and Planetary Science Letters*, 9:225–231.

Kurat, G., G. Hoinkes, and K. Fredriksson
1975. Zoned Ca-Al-rich Chondrule in Bali: New Evidence against the Primordial Condensation Model. *Earth and Planetary Science Letters*, 26:140–144.

Lord, H.C. III
1965. Molecular Equilibria and Condensation in a Solar Nebula and Cool Stellar Atmospheres. *Icarus*, 4:279–288.

Lorin, J.C., and M. Christophe Michel-Lévy
1978. Heavy Rare Metals and Magnesium Isotopic Anomalies Studies in Allende and Leoville Calcium-Aluminum Rich Inclusions. In *Lunar Science, IX*, pages 660–662. Houston: Lunar and Planetary Institute.

Marvin, U.B., J.A. Wood, and J.S. Dickey
1970. Ca-Al-rich Phases in the Allende Meteorite. *Earth and Planetary Science Letters*, 7:346–350.

Mason, B.
1974. Aluminum-Titanium-rich Pyroxenes, with Special Reference to the Allende Meteorite. *American Mineralogist*, 59:1198–1202.

Mason, B., and P.M. Martin
1974. Minor and Trace Element Distribution in Melilite and Pyroxene from the Allende Meteorite. *Earth and Planetary Science Letters*, 22:141–144.
1977. Geochemical Differences among Components of the Allende Meteorite. *Smithsonian Contributions to the Earth Sciences*, 19:84–95.

Niederer, F.R., D.A. Papanastassiou, and G.J. Wasserburg
1980. Titanium Isotope Anomalies in Allende Inclusions. *Meteoritics*, 15:339, 340.
1981. The Isotopic Composition of Titanium in the Allende and Leoville Meteorites. *Geochimica et Cosmochimica Acta*, 45:1017–1031.

Niemeyer, S., and G.W. Lugmair
1980. Ti Isotope Anomalies in "Un-FUN" Allende Inclusions. *Meteoritics*, 15:341.

Simon, S.B., and S.E. Haggerty
1980. Bulk Compositions of Chondrules in the Allende Meteorite. In *Proceedings of the Eleventh Lunar and Planetary Science Conference*, pages 901– 927. New York: Pergamon Press.

Steele, I.M., and I.D. Hutcheon
1979. Anatomy of Allende Inclusions: Mineralogy and Mg Isotopes in Two Ca-Al-rich Inclusions. In *Lunar and Planetary Science, X*, pages 1166–1168. Houston: Lunar and Planetary Institute.

Tanaka, T., and A. Masuda
1973. Rare-Earth Elements in Matrix, Inclusions, and Chondrules of the Allende Meteorite. *Icarus*, 19:523–530.

Taylor, S.R.
1965. Geochemical Analysis by Spark Source Mass Spectrography. *Geochimica et Cosmochimica Acta*, 29: 1243–1261.
1971. Geochemical Applications of Spark Source Mass Spectrography, II: Photoplate Data Processing. *Geochimica et Cosmochimica Acta*, 35:1187–1196.

Taylor, S.R., and M.P. Gorton
1977. Geochemical Application of Spark Source Mass Spectrography, III: Element Sensitivity, Precision

and Accuracy. *Geochimica et Cosmochimica Acta*, 41:1375–1380.

Taylor, S.R., and B. Mason
1978. Chemical Characteristics of Ca-Al Inclusions in the Allende Meteorite. In *Lunar and Planetary Science, IX*, pages 1158–1160. Houston: Lunar and Planetary Institute.

Wänke, H., H. Baddenhausen, H. Palme, and B. Spettel
1974. On the Chemistry of the Allende Inclusions and Their Origin As High Temperature Condensates. *Earth and Planetary Science Letters*, 23:1–7.

Wark, D.A.
1981a. Alteration and Metasomatism of Allende Ca-Al-rich Materials. In *Lunar and Planetary Science, XII*, pages 1145–1147. Houston: Lunar and Planetary Institute.
1981b. The Pre-Alteration Compositions of Allende Ca-Al-rich Condensates. In *Lunar and Planetary Science, XII*, pages 1148–1150. Houston: Lunar and Planetary Institute.

Wark, D.A., and J.F. Lovering
1980. More Early Solar System Stratigraphy: Coarse-grained CAIs. In *Lunar and Planetary Science, XI*, pages 1208–1210. Houston: Lunar and Planetary Institute.

Wasserburg, G.J., and J.C. Huenke
1979. I-Xe Dating of I-bearing Phases in Allende. In *Lunar and Planetary Science, X*, pages 1307-1309. Houston: Lunar and Planetary Institute.

Wood, J.A.
1981. The Interstellar Dust As a Precursor of Ca,Al-rich Inclusions in Carbonaceous Chondrites. *Earth and Planetary Science Letters*, 56:32–44.

Yoder, H.S., and T. Sahama
1957. Olivine X-ray Determinative Curve. *American Mineralogist*, 42:475–491.